A peer-reviewed version of this preprint was published in PeerJ on 18 January 2016.

Foth C, Hedrick BP, Ezcurra MD. 2016. Cranial ontogenetic variation in early saurischians and the role of heterochrony in the diversification of predatory dinosaurs. PeerJ 4:e1589 https://doi.org/10.7717/peerj.1589

Cranial ontogenetic variation in early saurischians and the role of heterochrony in the diversification of predatory dinosaurs

Foth Christian, Brandon P Hedrick, Martin D Ezcurra

Non-avian saurischian skulls underwent at least 165 million years of evolution and shapes varied from elongated skulls, such as in *Coelophysis*, to short and box-shaped skulls, such as in *Camarasaurus*. A number of factors have long been considered to drive skull shape, including phylogeny, dietary preferences and functional constraints. However, heterochrony is increasingly being recognized as a major factor in dinosaur evolution. In order to quantitatively analyse the impact of heterochrony on saurischian skull shape, we have analysed five ontogenetic trajectories using two-dimensional geometric morphometrics in a phylogenetic framework. This allowed for the evaluation of how heterochrony affected overall skull shape through both ontogenetic and phylogenetic trajectories and how it impacted modular changes within the skull. Using principal component analyses and multivariate regressions, it was possible to quantify different ontogenetic trajectories in light of heterochrony. The results recovered here indicate that taxa underwent a combination of local paedomorphosis and peramorphosis within the skull along individual ontogenies and phylogenies, but that either peramorphosis or paedomorphosis dominated when the skull was considered as a whole. We found that the hypothetical ancestor of Saurischia led to basal Sauropodomorpha mainly through paedomorphosis, and to Neotheropoda mainly through peramorphosis. Paedomorphosis then led from Orionides to Avetheropoda, indicating that the paedomorphic trend previously found in advanced coelurosaurs may extend back into the early evolution of Avetheropoda. Not only are changes in saurischian skull shape complex due to the large number of factors that affect shape, but heterochrony itself is complex, with a number of reversals throughout non-avian saurischian evolution. The sampling of ontogenetic trajectories is considerably lower than the sampling of adult species and the current study represents a first exploratory analysis. To better understand the impact of heterochrony on cranial evolution in saurischians, the data set we present must be expanded and complemented with further sampling from future fossil discoveries, especially of juvenile taxa.

PeerJ PrePrints | https://dx.doi.org/10.7287/peerj.preprints.1185v1 | CC-BY 4.0 Open Access | rec: 18 Jun 2015, publ: 18 Jun 2015

Cranial ontogenetic variation in early saurischians and the role of heterochrony in the diversification of predatory dinosaurs

Christian Foth[1,2,3], Brandon P. Hedrick[4], Martín D. Ezcurra[2,5,6]

[1] SNBS, Bayerische Staatssammlung für Paläontologie und Geologie, Richard Wagner-Str. 10, D-80333 München

[2] Department of Earth and Environmental Sciences, Ludwig-Maximilians-Universität, Richard-Wagner-Str. 10, D-80333 München, Germany

[3] Department of Geosciences, University of Fribourg/Freiburg, Chemin du Musée 6, 1700 Fribourg, Switzerland

[4] Department of Earth and Environmental Science, University of Pennsylvania, 251 Hayden Hall, 240 S 33rd Street, Philadelphia, PA 19104, USA

[5] School of Geography, Earth and Environmental Sciences, University of Birmingham, Edgbaston, Birmingham B15 2TT, UK

[6] Sección Paleontología de Vertebrados, Museo Argentino de Ciencias Naturales "Bernardino Rivadavia", Buenos Aires C1405DJR, Argentina

Correspondence: Christian Foth, Department of Geosciences, University of Fribourg/Freiburg, Chemin du Musée 6, 1700 Fribourg, Switzerland

Tel.: +41 26 300 8944

e-mail: christian.foth@gmx.net

24 **Short title: Heterochrony in early saurischian skulls**

Abstract

Non-avian saurischian skulls underwent at least 165 million years of evolution and shapes varied from elongated skulls, such as in *Coelophysis*, to short and box-shaped skulls, such as in *Camarasaurus*. A number of factors have long been considered to drive skull shape, including phylogeny, dietary preferences and functional constraints. However, heterochrony is increasingly being recognized as a major factor in dinosaur evolution. In order to quantitatively analyse the impact of heterochrony on saurischian skull shape, we have analysed five ontogenetic trajectories using two-dimensional geometric morphometrics in a phylogenetic framework. This allowed for the evaluation of how heterochrony affected overall skull shape through both ontogenetic and phylogenetic trajectories and how it impacted modular changes within the skull. Using principal component analyses and multivariate regressions, it was possible to quantify different ontogenetic trajectories in light of heterochrony. The results recovered here indicate that taxa underwent a combination of local paedomorphosis and peramorphosis within the skull along individual ontogenies and phylogenies, but that either peramorphosis or paedomorphosis dominated when the skull was considered as a whole. We found that the hypothetical ancestor of Saurischia led to basal Sauropodomorpha mainly through paedomorphosis, and to Neotheropoda mainly through peramorphosis. Paedomorphosis then led from Orionides to Avetheropoda, indicating that the paedomorphic trend previously found in advanced coelurosaurs may extend back into the early evolution of Avetheropoda. Not only are changes in saurischian skull shape complex due to the large number of factors that affect shape, but heterochrony itself is complex, with a number of reversals throughout non-avian saurischian evolution. The sampling of ontogenetic trajectories is considerably lower than the sampling of adult species and the current study represents a first exploratory analysis. To better understand the impact of heterochrony on

cranial evolution in saurischians, the data set we present must be expanded and complemented with further sampling from future fossil discoveries, especially of juvenile taxa.

Keywords

Dinosauria, Sauropodomorpha, Theropoda, skull shape, ontogeny, heterochrony, evolution, geometric morphometrics

Introduction

Heterochrony describes evolutionary changes due to shifts in the timing or rate of developmental processes in an organism relative to the respective processes in its ancestor (Alberch *et al.*, 1979; McNamara, 1982, 2012; Reilly, Wiley & Meinhardt, 1997; Klingenberg, 1998; McNamara & McKinney, 2005). Heterochrony can lead to significant evolutionary changes in body plans within relatively short periods of time. Two major types of heterochronic processes are discerned: paedomorphosis and peramorphosis. Paedomorphosis occurs when the later ontogenetic stages of an organism retain characteristics from earlier ontogenetic stages of its ancestor, whereas a peramorphic organism is ontogenetically more developed than the later ontogenetic stages of its ancestor (Klingenberg, 1998). In practice, evidence for heterochronic events in evolution can be detected by comparing the ontogenetic trajectories of different taxa under the consideration of their phylogenetic interrelationships.

Documentation of heterochrony in the vertebrate fossil record is limited. Preserved fossil ontogenetic series are rare due to the fact that early juvenile specimens are either lacking or incomplete. Nevertheless, the role of heterochrony has been recognized and discussed for the

evolution of multiple fossil lineages that do preserve ontogenetic series (Gerber, Neige & Eble, 2007; Schoch, 2009, 2010, 2014; Bhullar, 2012; Forasiepi & Sánchez-Villagra, 2014; Ezcurra & Butler, 2015), including non-avian dinosaurs (e.g. Long & McNamara, 1997; Erickson *et al.*, 2004; Guenther, 2009; Bhullar *et al.*, 2012; Canale *et al.*, 2014). For example, Long & McNamara (1997), Erickson *et al.* (2004) and Canale *et al.* (2014) hypothesized that the evolution of large body size in carcharodontosaurids and tyrannosaurids from medium-sized ancestors was the result of peramorphosis. Further, Bhullar *et al.* (2012) proposed that the skull shape of recent birds was the result of paedomorphic changes from both non-avian theropods and early birds, such as *Archaeopteryx* and Enantiornithes.

Shape diversity in non-avian dinosaurs has recently become a popular research venue, in which geometric morphometric methods have been applied on a regular basis (e.g. Bonnan, 2004; Chinnery, 2004; Campione & Evans, 2011; Hedrick & Dodson, 2013; Lautenschlager, 2014; Schwarz-Wings & Böhm, 2014; Maiorino *et al.*, 2015). Skull shape diversity in saurischian dinosaurs has been studied in particular detail (e.g. Young & Larvan, 2010; Rauhut *et al.*, 2011; Brusatte *et al.*, 2012; Bhullar *et al.*, 2012; Foth & Rauhut, 2013a,b), but usually in relation to functional constraints, dietary preferences, phylogenetic interrelationships, and macroevolutionary patterns. Geometric morphometrics is a powerful method to quantify both intraspecific (e.g. ontogeny, sexual dimorphism, polymorphism) and interspecific (e.g. systematics, macroevolution) shape variation on the basis of homologous landmarks or outlines (Corti, 1993; Rohlf & Marcus, 1993; Adams, Rohlf & Slice, 2004; Slice, 2007; Mitteroecker & Gunz, 2009; Zelditch, Swiderski & Sheets, 2012). As a result, geometric morphometrics has also been successfully applied to the study of heterochrony among various tetrapod groups (e.g.

Berge & Pennin, 2004; Mitteroecker *et al.*, 2004; Mitteroecker, Gunz & Bookstein, 2005; Liebermann *et al.*, 2007; Drake, 2011; Piras *et al.*, 2011; Bhullar *et al.*, 2012). However, only Bhullar *et al.* (2012) have examined cranial shape diversity in theropod dinosaurs in the context of heterochrony.

The aim of the current study is to investigate the cranial shape diversity of saurischian dinosaurs by comparing the ontogenetic trajectories of different taxa from both qualitative and quantitative data, using two-dimensional geometric morphometrics (2D GM). Phylogenetic relationships of the taxa sampled in this study are taken into account and integrated into an ancestor-descendant framework to look for possible heterochronic processes in the cranial evolution of saurischians. However, due to the limited number of ontogenetic series known for sauropodomorphs, the current study focuses primarily on the early evolution of theropods. Therefore, this study is a first exploratory investigation of heterochrony in basal saurischians, which will need to be expanded and complemented with further sampling from future fossil discoveries.

Materials and Methods

Institutional Abbreviations

BMMS, Bürgermeister Müller Museum Solnhofen, Solnhofen, Germany; **CM**, Carnegie Museum of Natural History, Pittsburgh, USA; **GR**, Ruth Hall Museum, Ghost Ranch, USA; **IVPP**, Institute of Vertebrate Paleontology and Paleoanthropology, Beijing, China, **MCZ**, Museum of Comparative Zoology, Harvard University, USA.

Taxon sampling

We sampled the crania of 35 saurischian dinosaur taxa (10 sauropodomorphs and 25 non-pennaraptoran theropods, see Table S3 in the Supplementary Information) on the basis of published reconstructions of adult (or advanced subadults) individuals in lateral view (with exception of the reconstructions of the basal tyrannosauroid *Dilong* [IVPP V14243] and the basal alvarezsauroid *Haplocheirus* [IVPP V15988], which were based on our personal observations). Large nasal crests of several theropods (e.g. *Ceratosaurus*, *Dilophosaurus*, *Guanlong*) were found to have an important impact on the ancestral shape reconstruction (see below) of Averostra, Avetheropoda, Coelurosauria and Tyrannosauroidea (see Fig. S5, Table S8, S9 in the Supplementary Information). Although cranial crests are a common structure within theropod dinosaurs (Molnar, 2005), reconstruction of moderately to strongly crested hypothetical ancestors within this study would necessarily be artificial due to the lack of intermediate crested forms and relatively small sample size of the available data set. As a result, *Ceratosaurus*, *Dilophosaurus* and *Guanlong* were not included in the main sample.

Monolophosaurus was the only crested taxon included in the main data set because it possesses a rather moderately sized and simple nasal crest. '*Syntarsus' kayentakatae*, which is often reconstructed with a pair of prominent nasal crests (Rowe, 1989; Tykoski, 1998), was analysed in this study without crests since this structure is probably artificial due to post-mortem displacement of the nasals (Ezcurra & Novas, 2005, 2007). As cranial crests usually represent external visual signal structures (Sampson, 1999; Padian & Horner, 2011; Hone, Naish & Cuthill, 2012), their evolutionary development was most likely sourced from regional peramorphic processes (see discussion on the evolution of horns and frills in Ceratopsia by Long

& McNamara 1997). We generated a second data set that includes crested taxa for comparison with the main data set (see below).

In our sample, five taxa preserve early ontogenetic stages allowing the reconstruction of both juvenile and adult skull shapes, which were used to reconstruct five simplified (i.e. including two stages) ontogenetic series. This sample includes the basal sauropodomorph *Massospondylus* (ontogenetic outgroup trajectory), the basal theropod *Coelophysis*, the megalosaurid *Dubreuillosaurus*, the allosauroid *Allosaurus*, and the basal coelurosaur *Tarbosaurus*. As the fossil record of juvenile dinosaur specimens with complete skull material is rare, the number of ontogenetic series is limited. To improve the sampling, previous studies have included reconstructions from multiple partial juvenile skulls or juveniles from closely related taxa (e.g. Bhullar *et al.*, 2012). We implemented this approach in two cases: the reconstruction of the juvenile *Coelophysis* sample was based on three incomplete, somewhat taphonomically deformed individuals (MCZ 4326; GR 392; CM 31375); and *Sciurumimus* (BMMS BK 11) was used as the juvenile representative of megalosaurids (e.g. *Dubreuillosaurus*) (see Rauhut *et al.*, 2012). In contrast to Bhullar *et al.* (2012), we did not include the ontogenetic series of *Byronosaurus*, Therizinosauridae (represented by a therizinosaurid embryo and the skull of *Erlikosaurus*) and *Compsognathus* in the data set because the postorbital region of the juvenile skulls of the former two taxa is crushed or incomplete (Bever & Norell, 2009; Kundrát *et al.*, 2009), and the taxonomic referral of *Scipionyx* (as juvenile taxon) to the clade Compsognathidae (see Dal Sasso & Maganuco, 2011) is uncertain (see Rauhut *et al.*, 2012).

Two-dimensional Geometric Morphometrics (2D GM)

We used 20 landmarks (LMs) and 51 semi-landmarks (semi-LMs) on our sample in order to accurately capture skull shape. The landmarks were collected using the software tpsDig2 (Rohlf, 2005) and were classified as either type 1 (points where two bone sutures meet) or type 2 (points of maximum curvature and extremities) (Bookstein, 1991) (see Fig. S1, Table S1 in the Supplementary Information for full description). Type 3 landmarks (points constructed between two homologous landmarks, which mainly define the shape of the skull or skull openings rather than the position of exact homologous points) were not used in our study. Semi-landmarks were used to capture the shape of skull openings and the overall skull outline by defining a number of points that are placed equidistantly along respective curves (Bookstein, 1991; Bookstein *et al.*, 1999). The percent error for digitizing landmarks and semi-landmarks by hand was estimated for the skull reconstruction of the juvenile *Coelophysis* (with n = 10 replications) using the method described by Singleton (2002). Landmark and semi-landmark error varies between 0.117 percent (LM 51 - most posterior point of the descending process of the maxilla contacting the nasal and/or the lacrimal) and 0.738 percent (LM 3 - contact between the maxilla and jugal along the ventral margin of the skull) with a mean of 0.283 percent. The error has no significant effect on the shape analyses (see Table S2 in the Supplementary Information).

The shape coordinates were then imported into the software package MorphoJ 1.05d (Klingenberg, 2011) and were superimposed using generalized Procrustes analysis (GPA). GPA rotates, translates and resizes all specimens accounting for all non-shape related differences between landmark configurations, leaving only shape information (Gower, 1975; Rohlf & Slice, 1990). Although semi-landmarks have fewer degrees of freedom than regular landmarks (and thus contain less shape information) (Bookstein, 1991), we treated landmarks and semi-

landmarks as equivalent for GPA (Zelditch, Swiderski & Sheets, 2012) and did not slide the semi-landmarks. The sliding process created considerable artificial deformation on the Procrustes shape in some taxa (see Fig. S2 in the Supplementary Information). However, due to the equivalent weighting of landmarks and semi-landmarks, it should be kept in mind that the shape information captured by the semi-landmarks strongly influences the results (Zelditch, Swiderski & Sheets, 2012; see below). The generated Procrustes shapes were used to compare juvenile and adult skull shapes to each other in each ontogenetic series to find ontogenetic patterns between and within taxa.

The resulting Procrustes coordinates were subjected to an exploratory principal components analysis (PCA) using the covariance matrix generated from Procrustes coordinates. PCA simplifies descriptions of variation among individuals by creating new sets of variables that are linear combinations of the original set such that the new sets are independent of one another and have zero covariance. The principal components (PCs) describe successively smaller amounts of total variance of the sample. This allows for a larger proportion of the variance to be described using a smaller number of variables than the original data would have allowed (Zelditch, Swiderski & Sheets, 2012). The different ontogenetic series were compared to each other by calculating pairwise two-dimensional angles between different trajectories based on the PC values of the first three axes, which are the significant principal components (significance calculated using the broken stick method, see Jackson, 1993). PCs 1, 2 and 3 together contain 68% of the total shape variation. Each ontogenetic trajectory was described as a phenotypic change vector, $\Delta \vec{y}_i = \vec{y}_{ij} - \vec{y}_{ik}$, with two shape traits (PC 1 vs. PC 2 and PC 1 vs. PC 3), where *i* is a specific ontogeny between two fixed stages, juvenile (*j*) and adult (*k*) (Collyer & Adam, 2007).

The difference in direction (angle) between the ontogenetic phenotypic change vectors $\Delta \vec{y}_a, \Delta \vec{y}_b$ was calculated using the dot product $\cos^{-1}(\Delta \vec{y}_a, \Delta \vec{y}_b) = \frac{\Delta \vec{y}_a \cdot \Delta \vec{y}_b}{|\Delta \vec{y}_a||\Delta \vec{y}_b|}$.

A multivariate regression of the Procrustes coordinates against log-transformed centroid sizes (= square root of the sum of the squared distances of each landmark to the centroid of the landmark configuration, Zelditch, Swiderski & Sheets, 2012) were used to test if overall skull shape variation is correlated to size and also to compare the different ontogenetic trajectories in terms of heterochrony (Piras et al., 2011; Bhullar et al., 2012; Zelditch, Swiderski & Sheets, 2012). As heterochrony is defined as the change in the timing or rate of developmental processes in ancestor-descendant relationships (Alberch *et al*., 1979; Klingenberg, 1998; McNamara, 2012), a direct comparison of ontogenetic trajectories from different species (as terminal taxa) can be problematic because it is hard to determine which trajectory would represent the ancestral and the descendant form, respectively. This is exacerbated when the supposed ancestral (terminal) species possesses an unknown, long evolutionary history resulting from a ghost lineage. This problem can be partially solved using a phylogenetic approach, in which the ancestor of two sister (terminal) taxa is represented by the hypothetical last common ancestor (Hennig, 1966). Therefore, we calculated hypothetical ancestral ontogenetic trajectories for Saurischia, Neotheropoda, Orionides and Avetheropoda using ancestral shape reconstructions as follows (see Fig. S3, S4 in the Supplementary Information). An informal supertree including all adult taxa was created based on recent phylogenetic analyses (see Fig. S3, S4 in the Supplementary Information): basal Sauropodomorpha (Cabreira *et al*., 2011), Coelophysoidea (Ezcurra & Novas, 2007), Ceratosauria (Pol & Rauhut, 2012), Tetanurae (Carrano, Benson & Sampson, 2012), and Coelurosauria (Turner *et al*., 2012; Loewen *et al*., 2013). The phylogenetic position

of *Eoraptor* follows Martínez *et al.* (2011) and Martínez, Apaldetti & Abelin (2013). The position of *Adeopapposaurus* as sister taxon of *Massospondylus* follows Martínez (2009). The position of *Herrerasaurus* and *Tawa* at the base of Theropoda is based on Sues *et al*. (2011). *Zupaysaurus* was placed outside Coelophysoidea as one of the successive sister taxa of Averostra (Smith *et al.*, 2007; Sues *et al*., 2011; Ezcurra, 2012). The supertree was time-calibrated using the stratigraphic age of each taxon (as mean of time interval) (see Table S3, S8 in the Supplementary Information). The assignment of branch lengths was performed in R (R Development Core Team, 2011) using the APE package (version 2.7-2; Paradis, Claude & Strimmer, 2004) and a protocol written by Graeme Lloyd (see http://www.graemetlloyd.com/methdpf.html) for adjusting zero branch lengths by sharing out the time equally between branches (see Brusatte *et al*., 2008; Brusatte, 2011), and adding an arbitrary length of 1 million years to the root. The time-calibrated supertree was imported into the software package Mesquite 2.72 (Maddison & Maddison, 2009). Subsequently, Procrustes coordinates and centroid sizes of the adult taxa were mapped onto the supertree as continuous characters using square change parsimony. This algorithm performs an ancestral state reconstruction by collating the sum of squared changes of continuous characters along all branches of a tree and estimates the most parsimonious ancestral states by minimizing the total sum of squared changes across the tree (Maddison, 1991). In the next step we tested if the continuous data contain a phylogenetic signal. We performed a permutation test in MorphoJ in which the topology was held constant and both the Procrustes shape data and the centroid size for each taxon were randomly permuted across the tree 10,000 times (Laurin, 2004; Klingenberg & Gidaszewski, 2010). The data contain a statistically significant phylogenetic signal if the squared length of the original supertree occurs in at least 95% of the randomly generated trees.

To obtain the ancestral ontogenetic trajectories, the protocol described above was repeated in a new nexus file containing the Procrustes shapes and centroid sizes of the juvenile taxa. As the juvenile data set is only represented by five taxa, the original supertree was pruned such that only these respective taxa remained, retaining the original time-calibration. Finally, the ancestral Procrustes shapes and centroid sizes of both juvenile and adult Saurischia, Neotheropoda, Orionides and Avetheropoda were exported and combined with the respective data from the ontogenetic trajectories of the terminal taxa. The ancestral Procrustes shape of Averostra was not considered because no ceratosaur juveniles have been published in detail so far (see Madsen & Welles, 2000). The new data set was loaded again into MorphoJ to perform a multivariate, pooled within-group regression of Procrustes shape against centroid size. Peramorphosis was inferred if the regression score of the descendant trajectory was higher than that of the respective ancestral one, whereas paedomorphosis resulted from a lower score. However, to test if the shape changes, and as a result the presence of heterochrony, of an ancestor-descendant relationship are statistically meaningful, we calculated the confidence interval (CI) of the regression scores of terminal and ancestral taxa (n = 69) and compared them with the differences of ancestral and descendant regression scores from the sub-sample containing the ontogenetic trajectories. Changes were considered significant if the differences between regression scores are at least 1.5 times higher than the CI value (see Cumming, Fidler & Vaux, 2007). The angles between ontogenetic trajectories were calculated based on Procrustes distances and centroid sizes (see above). To gain better insights into specific heterochronic changes, this procedure was repeated for the shape of several different skull regions, namely skull outline, external naris, maxilla,

antorbital fenestra, orbit, infratemporal fenestra, jugal-quadratojugal complex, postorbital, and skull roof, including the shape of the ventral process of the lacrimal.

In order to estimate the influence of the semi-landmarks (see above) on the shape data, a second data set was created that included only landmark data. The analyses on this data set (only for the overall skull shape) were performed as described above. Finally, the ancestral shape reconstructions calculated for the adult taxa were used to discuss the evolutionary changes within basal Sauropodomorpha and Theropoda with respect to the ontogenetic changes and heterochronic trends found in the different trajectories.

Results

General ontogenetic changes

The juveniles of the sauropodomorph *Massospondylus* and the theropods that were sampled here tend to have skulls with a short and abruptly tapering snout, short antorbital fenestra, large subcircular orbits, slender jugals, and dorsoventrally deep orbital and postorbital regions relative to the snout. In addition, the jaw joint is more anteriorly placed relative to the occiput, with exception of the juvenile specimen of *Allosaurus* sampled here. The general ontogenetic pattern includes an elongated and dorsoventrally deeper snout relative to the orbital and postorbital regions, and also a relative increase in size of the antorbital fenestra, which correlates with a relative decrease in size of the orbit. Finally, the jugal becomes more massive in all taxa, which is more pronounced in the large-bodied theropods *Allosaurus* and *Tarbosaurus* (Fig. 1). The relative elongation of the snout and antorbital fenestra were not observed in the *Allosaurus* or *Tarbosaurus* ontogenies, which is probably due to the fact that the juveniles sampled do not

represent the earliest ontogenetic stages (Loewen, 2009; Tsuihiji *et al.*, 2011, see discussion). However, the discovery of an isolated maxilla identified as a hatchling allosauroid might indicate that the snout of early *Allosaurus* juveniles was probably short and subsequently increased in relative length during early ontogeny (Rauhut & Fechner, 2005).

Principal component analysis and phylogenetic correlation

The first three principal components account for 68.0% of the total variation (PC 1: 30.8 %; PC 2: 23.9 %; PC 3: 13.3 %), in which PC 2 and PC 3 contain the main allometric shape information (see Table S16 in the Supplementary Information). PC 1 describes the overall skull depth, size and anteroposterior position of the external naris, length of the premaxilla, size of the maxillary antorbital fossa, and position of the lacrimal and postorbital in the anteroposterior axis (affecting the size of the antorbital fenestra, orbit and infratemporal fenestra). The dorsoventral dimension of the orbit is affected by the relative depth of the entire orbital and postorbital regions, while that of the infratemporal fenestra is affected by the relative position of the jugal-quadratojugal bar. The variation in the depth of the skull also affects the position of the jaw joint in the dorsoventral axis.

PC 2 describes the length of the snout caused by variation in the length of the maxilla and inclination and anteroposterior position of the lacrimal. The inclination of the lacrimal affects the size of the antorbital fenestra, while both position and inclination affect the anteroposterior dimension of the orbit. PC 2 also accounts for the length and the dorsoventral position of the external naris and size of the upper temporal region.

PC 3 describes the length of the premaxilla, posterior extension of the external naris, dorsoventral height of the maxilla, and anteroposterior dimension of the ventral process of the lacrimal (which affects the shape of the antorbital fenestra and orbit). The shape of the orbit is further affected by the anteroposterior dimension of the jugal-postorbital bar. Further variation captured by PC 3 is related to the shape of the skull roof in the orbital and postorbital regions, dorsoventral height of the infratemporal fenestra, and position of the jaw joint in the anterodorsal-posteroventral axis.

The permutation tests recovered that both Procrustes shapes (tree length weighted by branch lengths = 0.5108, $p < 0.0001$) and centroid size (tree length weighted by branch lengths = 8.3598, $p = 0.0005$) are correlated with phylogeny. The phylogenetic signal remains when semi-landmarks are excluded (tree length weighted by branch lengths = 0. 5341, $p < 0.0001$) and when crested taxa are included (tree length weighted by branch lengths = 0.5 482, $p < 0.0001$) in the sample.

Ontogenetic trajectories in the principal component morphospace

The ontogenetic trajectory of *Allosaurus* is mainly explained by shape variation captured by PC 1. The ontogenetic trajectory of *Coelophysis* is mainly explained by the shape variation captured by PCs 1 and 2, and that of *Tarbosaurus* is mainly explained by the shape variation captured by PCs 1 and 3. The ontogenetic trajectory of *Coelophysis* is in the opposite direction along PC 1 compared to the trajectories of *Allosaurus* and *Tarbosaurus*. The ontogenetic trajectories of *Massospondylus* and the megalosaurid taxon are mainly influenced by the shape variation captured by PCs 2 and 3, in which the ontogenetic trajectory of *Massospondylus* is directed in

345 the opposite direction along PC 3 to that of the megalosaurid taxon and *Tarbosaurus* (Fig. 2,
346 Table S4 in the Supplementary Information).
347
348 It should be noted that the directions of the ontogenetic trajectories do not change when crested
349 taxa are included in the data set (PC 1: 28.6 %; PC 2: 22.7 %; PC 3: 13.0 %; see Fig. S6, Table
350 S10, S11, S16, see Supplementary Information for results when crested taxa are included). By
351 contrast, the exclusion of semi-landmarks from the data set leads to five differently directed
352 ontogenetic trajectories (PC 1: 28.4 %; PC 2: 20.0 %; PC 3: 15.6 %). Excluding semi-landmarks,
353 the ontogenetic trajectory of the megalosaurid taxon is explained approximately equally by the
354 first three PCs, that of *Allosaurus* is mainly captured by PC 1 and 2, and that of *Tarbosaurus* is
355 explained by PCs 1 and 3. The ontogenetic trajectories of *Massospondylus* and *Coelophysis* are
356 mainly explained by shape variation captured by PCs 2 and 3, in which the ontogenetic trajectory
357 of *Massospondylus* along PC 3 is directed opposite to that of *Coelophysis*, *Tarbosaurus* and the
358 megalosaurid taxon (see Fig. S7, Table S12, S13 in the Supplementary Information with results
359 excluding semi-landmarks). Semi-landmark curves include important shape information and
360 their exclusion leads to missing informative data (e.g. skull outline) and as a result we will
361 discuss it below in the context of a sensitivity analysis.
362
363 Based on the results of the original data set (i.e. including semi-landmarks), the general
364 ontogenetic patterns described above are not completely uniform for all taxa (Figs. 1, 2). The
365 ontogenetic elongation of the snout is primarily related to a relative increase in the length of the
366 maxilla (PCs 1, 2). In *Massospondylus* and the megalosaurid taxon the ontogenetic elongation of
367 the snout is further affected by the relative increase of the length of the premaxilla (PC 3). The

relative increase in snout depth results mainly from a ventral expansion of the maxilla, which is more prominent in *Allosaurus* and *Tarbosaurus* than in other taxa (PCs 1, 3). In the megalosaurid taxon and *Allosaurus,* maxillary deepening occurs together with a dorsoventral expansion of the nasal (PC 1). Additionally, dorsoventral expansion of the premaxilla is observed in *Allosaurus* and *Tarbosaurus* (PC 1). The relative elongation of the snout in *Massospondylus*, the megalosaurid taxon and *Coelophysis* correlates with a relative increase in the anteroposterior length of the antorbital fenestra, caused by a posterior shift of the lacrimal and elongation of the maxilla (PCs 1, 2). Additionally, in *Coelophysis* the anterior border of the antorbital fenestra extends anteriorly (PC 1). In both *Massospondylus* and the megalosaurid taxon, the antorbital fenestra is shifted posteriorly during ontogeny (PC 2). The megalosaurid taxon shows a further dorsal expansion of the antorbital fenestra (PC 3), not seen in the latter two taxa. Although no relative size changes could be observed in the antorbital fenestrae of *Allosaurus* and *Tarbosaurus*, the antorbital fenestra of *Allosaurus* shifts posterodorsally during ontogeny, whereas that of *Tarbosaurus* shifts ventrally. In most trajectories, the most anterior point of the antorbital fossa shifts posteriorly during ontogeny (PCs 1−3), but a relative decrease in the length of the maxillary antorbital fossa is present in *Allosaurus* and *Tarbosaurus* (PC 1). In the megalosaurid taxon, the anterior margin of the antorbital fossa shifts ventrally, whereas in *Coelophysis* it shifts anteriorly (PC 1), which correlates with the anterior extension of the antorbital fenestra in this taxon (see above). As mentioned above, the orbit decreases in relative size in all taxa during ontogeny (PCs 1−3). In *Coelophysis* and *Massospondylus* this is related to a relative shift of the lacrimal posteriorly (PCs 1, 2). In the megalosaurid taxon, *Allosaurus* and *Tarbosaurus* the relative size reduction is correlated with a change in orbital shape from subcircular to oval. In the megalosaurid taxon these changes are linked to a posterior shift of the

lacrimal (PC 2) and anterior shift of the postorbital and ascending process of the jugal (PC 3), which is correlated with an anterior extension of the infratemporal fenestra. In *Allosaurus*, the ontogenetic changes of the orbit are related to the posterior extension of the lacrimal and anterior shift of the postorbital and ascending process of the jugal (PC 1). Additionally, the orbit of *Allosaurus* is shifted slightly dorsally. In *Tarbosaurus*, these changes result from an anterior extension of both the postorbital and ascending process of the jugal (PC 3). The orbit of *Tarbosaurus* becomes posteriorly constricted by an anterior shift of the ventral process of the postorbital, forming a suborbital process.

In addition to these more general ontogenetic modifications, the different trajectories of individual taxa show specific shape changes (Fig. 1):

a) In *Massospondylus* the external naris becomes larger and expands dorsally. The postorbital also becomes relatively more robust. The infratemporal fenestra decreases in relative size. The jaw joint moves anteroventrally.

b) In *Coelophysis* the external naris becomes smaller and shifts anteriorly. The notch of the alveolar margin between the premaxilla and maxilla decreases in relative size during ontogeny, while the alveolar margin of the premaxilla becomes more aligned with that of the maxilla. The descending process of the lacrimal becomes more slender anteroposteriorly. The postorbital becomes more gracile in its relative shape. The infratemporal fenestra increases in relative size. The jaw joint moves posterodorsally.

c) In the megalosaurid taxon, the external naris becomes relatively larger and expands posteriorly. The lacrimal is inclined strongly backwards and the postorbital becomes

relatively more robust. The infratemporal fenestra increases in its relative size. The jaw joint moves posteriorly.

d) In *Allosaurus* the external naris does not change in relative size, but shifts ventrally. The descending process of the lacrimal becomes more massive anteroposteriorly. The lacrimal develops a prominent dorsal horn through ontogeny. In contrast to previous taxa, the postorbital region of *Allosaurus* increases dorsoventrally such that the postorbital, quadratojugal and squamosal become more robust. The ventral shift of the jugal leads to the formation of a wide angle between the ventral margins of the maxilla and jugal. Due to its posteroventral expansion, the postorbital affects the overall shape of the infratemporal fenestra. However, the infratemporal fenestra does not decrease in its relative size, but shifts anteroventrally. The jaw joint moves anteroventrally.

e) In *Tarbosaurus* the external naris does not change in relative size, but shifts dorsally. As in *Allosaurus*, the descending process of the lacrimal becomes more massive. The same is true for the postorbital region, which increases in depth dorsoventrally. This change is correlated with the development of a more robust postorbital, quadratojugal and squamosal. The jaw joint moves posteroventrally.

Main heterochronic changes

Based on the multivariate, pooled within-group regression, peramorphic skulls tend to be more elongated, with long and slender snouts that have a rounded anterior end, and possess anteroposteriorly long antorbital fenestrae, oval orbits and a post-rostrum only slightly dorsoventrally higher than the snout. The maxilla increases in its relative length, but also expands ventrally. The ascending process of the maxilla, the anterior and ascending processes of

437 the jugal, and postorbital become more massive. Paedomorphic shape trends are opposite to
438 these peramorphic trends. All heterochronic processes are summarized in Figs. 2–7, Table 1, and
439 Table S6 and S7 in the Supplementary Information.
440
441 When compared to the hypothetical ancestor of Saurischia, the overall skull shape of
442 *Massospondylus* results from paedomorphosis primarily affecting the shape of the skull outline,
443 antorbital fenestra, orbit and skull roof. By contrast, the shapes of the external naris and
444 infratemporal fenestra of *Massospondylus* are peramorphic.
445
446 The evolutionary changes of overall skull shape that occurred from the hypothetical ancestor of
447 Saurischia to that of Neotheropoda are due to peramorphosis, which primarily affects the shape
448 of the skull outline, maxilla, antorbital fenestra, infratemporal fenestra and skull roof. Compared
449 to the hypothetical neotheropod ancestor, the skull of *Coelophysis* was found to be non-
450 significantly peramorphic. On the regional level, significant peramorphic shape changes found in
451 the external naris, antorbital fenestra and the skull roof. By contrast, significant shape changes
452 found in the orbit, postorbital, infratemporal fenestra, and jugal-quadratojugal complex are
453 influenced by paedomorphosis.
454
455 Between the hypothetical ancestors of Neotheropoda and Orionides (the hypothetical ancestor of
456 Averostra was not considered here) no significant shape changes could be observed for overall
457 skull shape. However, regional peramorphic changes are expressed significantly in the shape of
458 the external naris, maxilla, orbit, jugal-quadratojugal complex and postorbital. In comparison to
459 the hypothetical ancestor of Orionides, the skull of the megalosaurid taxon is peramorphic,

affecting all skull regions on a significant level except of antorbital fenestra and infratemporal fenestra.

Interestingly, the evolutionary changes in the overall skull shape that occurred from the hypothetical ancestor of Orionides to that of Avetheropoda are paedomorphic, affecting the shape of the skull outline, the external naris and the skull roof on a significant level.

Compared to the hypothetical ancestor of Avetheropoda, the overall skull shape of *Allosaurus* is peramorphic, but not on a significant level. On the regional level, *Allosaurus* shows significant changes related to peramorphosis in the maxilla, the orbit, the postorbital and the jugal-quadratojugal region. By contrast, the shape changes in the skull outline and external naris, which were found to be significant, are affected by paedomorphosis. The skull shape of *Tarbosaurus* was found to be non-significantly paedomorphic compared to the hypothetical ancestor of Avetheropoda. Regionally, significant paedomorphic changes are expressed in the shape of the skull outline, antorbital fenestra and skull roof. By contrast, the significant shapes found in the external naris, orbit, postorbital and jugal-quadratojugal complex are classified as peramorphic.

Peramorphosis found in the ontogenetic series is generally correlated with an increase in centroid size. Paedomorphosis observed in the hypothetical ancestor of Avetheropoda matches a decrease in centroid size, but not in *Massospondylus*.

When semi-landmarks are excluded from the data set, most of the heterochronic trends found in the sensitivity analysis are very similar to those described in the original analysis (see Fig. S7, Table S14, S15, S16, see Supplementary Information for results excluding semi-landmarks). However, contrasting with the main analysis, the evolutionary changes in the skull of *Massospondylus* are not significant with respect to the hypothetical ancestor of Saurischia, the skull of the hypothetical ancestor of Orionides is significantly peramorphic with respect to that of Neotheropoda, and the skull shape of *Tarbosaurus* is peramorphic compared to that of the hypothetical ancestor of Avetheropoda, but not significantly.

Discussion

Previous workers have hypothesized that skull shape diversity in theropods was driven by phylogenetic interrelationships, dietary preferences (Brusatte *et al*., 2012; Foth & Rauhut, 2013a), functional constraints (Henderson, 2002; Foth & Rauhut, 2013a), and also heterochrony (Long & McNamara, 1997; Bhullar *et al.*, 2012). The current study supports a strong influence of heterochrony on the cranial evolution of saurischian dinosaurs, which is indicated by different trajectories of morphological changes between the respective ontogenetic series. These changes are retained regardless of whether or not semi-landmarks or crested taxa are included in the sample. By comparing the ontogenetic trajectories in a hypothetical ancestor-descendant sequence, a complex pattern of heterochronic events is present within both the overall skull and different skull regions. The early evolution of sauropodomorphs is primarily affected by paedomorphosis, while shape changes in basal theropods is driven by peramorphosis. However, in more derived tetanurans (i.e. Avetheropoda, Coelurosauria) skull shape is predominantly affected by paedomorphosis (see also Bhullar *et al.*, 2012). When comparing different skull

regions with each other, it becomes clear that often both pera- and paedomorphic changes are modularly constrained, but one overall trend (either paedomorphosis or peramorphosis) is dominant for the entire skull.

Evolutionary changes in the skull shape of Sauropodomorpha

Based on the regression analysis of ontogenetic trajectories it is possible to determine which shape changes are related to paedomorphosis and which are related to peramorphosis (see above). This can be used to explain particular shape changes found between hypothetical ancestors and terminal taxa in the ancestral shape reconstruction analyses of the main sample (i.e. continuous character mapping of the Procrustes shapes) in terms of heterochrony. Comparing the skull shape of the hypothetical ancestor of Saurischia to that of Sauropodomorpha indicates an initial paedomorphosis in the evolution of the latter group, which is depicted by a decrease in the relative length of the preorbital region and an increase in the relative orbital size and depth of the postorbital region. However, the skull of the hypothetical ancestor of Massopoda is peramorphic with respect to that of Sauropodomorpha (but paedomorphic with respect to that of Saurischia, see above) due to a relative increase in length and depth of both the premaxilla and maxilla, as it was previously hypothesized by Long & McNamara (1997). The orbit size slightly decreases and becomes more oval, which was established as a peramorphic trend. Additionally, the jugal region becomes more massive. However, in Eusauropoda the snouts become more aberrant due to a dorsal shift of the external naris, posterodorsal extension of the premaxilla, elongation of the ascending process of the maxilla and modification of the postorbital region, affecting the relative size of the jugal and postorbital, which become more gracile (Wilson & Sereno, 1998; Rauhut *et al.*, 2011). While the

shape changes in the snout and the shift of the naris were diagnosed as peramorphic (Long & McNamara, 1997), one can assume on the basis of the current observations that the increase of gracility in the postorbital region of derived sauropods may result from modular paedomorphosis. However, this needs to be quantitatively analysed and is beyond the scope of the present study.

Evolutionary changes in the skull shape of Theropoda

The initial evolutionary changes in the skull shape of Theropoda were driven by peramorphic events, as is observed in the hypothetical ancestor of Neotheropoda and the megalosaurid taxon. These changes include the elongation of the snout, increase in length of the antorbital fenestra, and trends to a relatively smaller orbit and a more robust post-rostral region. In comparison to the ancestral reconstruction of Averostra, the skull of the hypothetical ancestor of Ceratosauria seems to be mainly the result of paedomorphosis, resulting in a shorter and deeper snout. The shape of the orbital and postorbital regions of *Limusaurus* (enlarged subcircular orbit and gracile jugal and postorbital) is paedomorphic with respect to the hypothetical ancestor of Averostra, while the respective regions in Late Cretaceous abelisaurids (e.g. *Carnotaurus* and *Majungasaurus*) are peramorphic (oval orbit, massive jugal and postorbital). The skull of the hypothetical ancestor of Avetheropoda is paedomorphic with respect to that of Orionides. This trend extends to the hypothetical ancestor of Coelurosauria, Maniraptoriformes and Maniraptora, leading to a shorter, more tapering snout in lateral view, smaller antorbital fenestra, enlarged subcircular orbit, and more gracile postrostral region, resembling the skull shape of the juvenile megalosaurid *Sciurumimus*. This finding may indicate that the paedomorphic trend hypothesized for Eumaniraptora (Bhullar *et al.*, 2012) probably reaches back into the early evolution of

Avetheropoda, and that basal coelurosaurs in fact represent "miniaturized" tetanurans, conserving juvenile characters in adult individuals. In contrast to this paedomorphic trend and to the results of regression analyses (see above), the ancestral shape reconstruction reveals that the skulls of allosauroids and tyrannosaurids become secondary more robust in relation to their respective ancestors, supporting convergent peramorphosis in both lineages (see Long & McNamara, 1997, Canale *et al*., 2014). This discrepancy to the regression results is probably linked to the incomplete sampling of ontogenetic trajectories in the regression analyses (see below). The heterochronic trends found in the current study are summarized in Fig. 8.

General comments on saurischian heterochrony

The cranial heterochronic events described here seem to be correlated with major trends observed in the evolution of body size in theropods and sauropodomorphs (Sander *et al*., 2010; Irmis, 2011; Dececchi & Larsson, 2013; Benson *et al*., 2014; Lee *et al*., 2014). As body size evolution itself is driven by heterochrony (Erickson *et al.*, 2004; Sander *et al*., 2004; McNamara, 2012), this correlation may indicate that the skull shape of theropods and sauropodomorphs is additionally influenced by body size evolution (i.e. heterochronic events in body size evolution can affect heterochrony in the cranium, but this correlation is not universal, see Therrien & Henderson, 2007; Bhullar *et al*., 2012), which is additionally indicated by the rough correlation found between heterochrony and centroid size.

Peramorphic trends in the cranial shape of Saurischia lead to skulls with an elongated snout, proportionally small and oval orbit, and robust postorbital region. On the other hand, paedomorphic trends tend to lead to skulls with short and deep snouts, enlarged subcircular

orbits and more gracile postorbital regions. These major differences in shape would clearly affect dietary preferences and functional constraints. The robust morphology of the postorbital region and the oval orbit in peramorphic skulls was previously discussed in relation to the generation of higher bite forces (Henderson, 2002; Foth & Rauhut, 2013a). However, these functional constraints go hand in hand with a decrease in cranial disparity (Brusatte *et al.*, 2012). Paedomorphic changes in the orbital and postorbital regions were discussed in relation to visual elaboration and brain enlargement (Bhullar *et al*., 2012), and may have played an important role for nocturnal activity (Schmitz & Motani, 2011) or the evolution of flight within Paraves (Balanoff *et al*., 2013). On the other hand, large and circular orbits might simply correlate with reduced mechanical stresses during biting (Henderson, 2002), which have been suggested to also influence size and shape of the external naris, antorbital fenestra and infratemporal fenestra (Witmer, 1997; Witzel & Preuschoft, 2005; Witzel *et al*., 2011).

Both ontogenetic and phylogenetic variations in snout shape are likely related to dietary preferences (Brusatte *et al.* 2012; Foth & Rauhut 2013), in which the shape of premaxillae and maxillae partly determines the number and size of teeth (Henderson & Weishampel, 2002). Various examples of ontogenetic changes in the morphology and number of teeth are documented in Saurischia, including the basal sauropodomorph *Massospondylus*, coelophysoids (Colbert, 1989), basal tetanurans (Rauhut & Fechner, 2005; Rauhut *et al.*, 2012), Tyrannosauridae (Carr, 1999; Tsuihiji *et al.*, 2011) and Maniraptora (Kundrát *et al*., 2008; Bever & Norell, 2009). Based on these observations the evolutionary increase in the number of teeth has been interpreted as peramorphic (Bever & Norell, 2009). Tooth morphology, however, was found to be a stronger indicator of diet than the shape of the snout itself (see Smith, 1993;

Barrett, 2000; Barrett, Butler & Nesbitt, 2011; Zanno & Makovicky, 2011; Foth & Rauhut, 2013a; Hendrickx & Mateus, 2014). In this context, Rauhut *et al.* (2012) hypothesised based on the similarities in the dentition of the juvenile megalosaurid *Sciurumimus*, adult compsognathids (Stromer, 1934; Currie & Chen, 2001; Peyer, 2006) and adult dromaeosaurids (Xu & Wu, 2001; Norell *et al.*, 2006), that strongly recurved crowns with reduced or no mesial serrations may be paedomorphic in the latter two taxa. This heterochrony probably results from the decrease of body size observed in coelurosaurs (see above) and indicate an evolutionary shift of dietary preferences to smaller prey (see also Zanno & Makovicky, 2011).

Limitations

As is common in vertebrate paleontology, the current study has a limited sample size when compared with extant neontological data sets (Brown & Vavrek, 2015). The current results are necessarily preliminary and must be viewed with some caution especially since the sampling of ontogenetic trajectories is considerably lower than the sampling of adult species. Furthermore, trajectories are constructed using a single juvenile and adult specimen, with no intermediate forms. The poor sample of juveniles is a result of rarity and poor preservation in the fossil record, which seems to be due to a number of factors, including preferred hunting of juveniles by predators (Hone & Rauhut, 2010) and a smaller likelihood of preservation, discovery, and collection because juveniles have smaller body sizes and more fragile bones than adults (Brown *et al.*, 2013). Another issue affecting our results is that the juvenile individuals sampled here are all of different early ontogenetic stages. The juvenile of *Massospondylus* still represents an embryo, which is close to hatching (Reisz *et al*., 2010); the megalosaurid taxon (i.e. *Sciurumimus albersdoerferi*) is an early juvenile and its exact age could not be determined (Rauhut *et al*.,

2012); the age of the *Coelophysis* juvenile reconstructed is approximately one year old (estimated by Colbert, 1990; Rinehart *et al*., 2009); the juvenile *Tarbosaurus* specimen is two to three years old (Tsuihiji *et al*., 2011); and the juvenile *Allosaurus* is likely five to seven years old (estimated on the basis of Bybee, Lee & Lamm, 2006; Loewen, 2009). Thus, it cannot be ruled out that the different ontogenetic stages of the juvenile specimens and the small number of individuals for each ontogenetic series have affected the progression of the calculated trajectories (and thus the angles between the trajectories) (see Cardini & Elton, 2007), including that of the hypothetical ancestors. Furthermore, due to small sample sizes, the statistical power of our analyses is generally low (see Cumming, Fidler & Vaux, 2007), limiting the explanatory power of our results. On the other hand, Brown & Vavrek (2015) recently demonstrated that the overall inference of allometry can be relatively robust against small sample sizes in both paleontological and neontological data sets, meaning that the current results probably still show a true, albeit statistically not well supported, signal. Due to this statistical uncertainty, further classification of heterochronic subtypes (e.g. neoteny or hypermorphosis) was avoided.

The (non-significant) paedomorphic trends found for *Tarbosaurus* in relation to the hypothetical ancestor of Avetheropoda illustrates the limitations of our analyses because this result is seemingly contradictory to previous hypotheses and the ancestral shape reconstruction, which proposed peramorphosis as the main driver of skull evolution in large-bodied tyrannosaurids (see above, Long & McNamara, 1997, Bhullar *et al.*, 2012). However, this result is most likely related to the small sample size of ontogenetic trajectories as skulls with elongated and slender snouts are considered to be peramorphic on the basis of the regression analyses. The hypothetical inclusion of more ontogenetic trajectories of large-bodied theropods would probably change this

result in favour of a trend towards a deeper snout. Furthermore, large-bodied tyrannosaurids like *Tarbosaurus* descended from small-bodied coelurosaurian ancestors (Xu *et al*., 2004, 2006; Brusatte *et al*., 2010; Rauhut *et al*., 2010; Benson *et al*., 2014), which means that the hypothetical inclusion of an ontogenetic trajectory of a small-bodied basal coelurosaur (e.g. *Compsognathus*, *Dilong*, *Haplocheirus*) and a respective hypothetical ancestor of Coelurosauria would probably change the current results, leading to a secondary peramorphic trend in Late Cretaceous tyrannosauroids, as previously recovered. Thus, this result is very likely an artefact of incomplete sampling.

Conclusions

The importance of heterochrony in non-avian dinosaur skull evolution is a relatively new concept. This is the first study to quantitatively assess the impact of skull heterochrony across early saurischian evolution. We analysed hypothetical ontogenetic trajectories of Saurischia, Neotheropoda, Orionides, and Avetheropoda using ontogenetic trajectories of *Massospondylus, Coelophysis,* a megalosaurid taxon, *Allosaurus*, and *Tarbosaurus*. General peramorphic skulls include more elongate and slender snouts, elongate antorbital fenestrae, oval orbits, dorsoventrally shallower post-rostral regions, and more massive maxillae, jugals, and postorbitals. Paedomorphic skulls show the opposite features. The shape changes from the hypothetical ancestor of Saurischia to *Massospondylus* were paedomorphic, while those from the hypothetical ancestor of Saurischia to Neotheropoda were peramorphic. Avetheropoda shows paedomorphic changes compared to Orionides, indicating that the paedomorphic trend hypothesised for Eumaniraptora may reach back into the early evolution of Avetheropoda. Different skull regions often show different trends: one region of the skull would be generally

peramorphic and another region would be predominantly paedomorphic, both along individual ontogenies and through phylogeny. We stress the importance of looking at morphometric data from different vantages to better elucidate trends. Though our data showed minimal differences between our crested-taxa and non-crested taxa data sets and semi-landmark and no semi-landmark data sets, it is important to fully evaluate all possible sources of trends, especially when working with a small data set. Our study is hampered by the preservation of the fossil record (mainly the poor sample of juvenile specimens) and more finds will help to elucidate evolutionary patterns related to heterochrony. With a larger number of taxa comprising juvenile and adult stages it will be possible to further test heterochronic hypotheses within Saurischia, and eliminate artefacts related to sample size. Future studies may also examine ontogenetic histories of individual taxa that have reasonably complete ontogenetic samples, such as *Coelophysis*, to evaluate which factors (dietary preference, heterochrony, etc.) drive shape change in individual taxa. A larger number of studies using geometric morphometrics for individual taxa as well as a more complete sampling within Saurischia are necessary to more completely assess the importance of heterochronic processes in both sauropodomorph and theropod skull shape. However, this study demonstrates that heterochrony played a large part in non-avian saurischian skull evolution.

Acknowledgements:

We thank Oliver Rauhut (Bayerische Staatssammlung für Paläontologie und Geologie, München), Miriam Zelditch (University of Michigan), Johannes Knebel (Ludwig Maximilians University, München) and Eduardo Ascarrunz (University of Fribourg) for discussion, and Michel Laurin (Sorbonne Universités, Paris) for critical comments on an earlier version of the

689 manuscript. We further thank Matthew Lamanna (Carnegie Museum of Natural History,
690 Pittsburgh), Alex Downs (Ruth Hall Museum, Ghost Ranch), David Gillette (Museum of
691 Northern Arizona, Flagstaff) and Xu Xing (Institute of Vertebrate Paleontology and
692 Paleoanthropology, Beijing) for access to collections. CF is supported by a DFG grant to Oliver
693 Rauhut (RA 1012/12-1) and a postdoctoral fellowship of the DAAD German Academic
694 Exchange Service (No. 9154678), BPH is supported by a Benjamin Franklin Fellowship at the
695 University of Pennsylvania, MDE is supported by a grant of the DFG Emmy Noether
696 Programme to Richard J. Butler (BU 2587/3-1).
697

698 **References**

699 Adams DC, Rohlf FJ, Slice DE. 2004. Geometric morphometrics: ten years of progress
700 following the "revolution." *Italian Journal of Zoology* 71:5–16.
701 Alberch P, Gould SJ, Oster GF, Wake DB. 1979. Size and shape in ontogeny and phylogeny.
702 *Paleobiology* 5:296–317.
703 Balanoff AM, Bever GS, Rowe TB, Norell MA. 2013. Evolutionary origins of the avian brain.
704 *Nature* 201:93–96.
705 Barrett PM. 2000. Prosauropod dinosaurs and iguanas: speculations on the diets of extinct
706 reptiles. In: Sues H-D ed. *Evolution of herbivory in terrestrial vertebrates*. Cambridge:
707 Cambridge University Press, 42–78.
708 Barrett PM, Butler RJ, Nesbitt SJ. 2011. The roles of herbivory and omnivory in early dinosaur
709 evolution. *Earth and Environmental Science Transactions of the Royal Society of*
710 *Edinburgh* 101:383–396.

711 Benson RBJ, Campione NE, Carrano MT, Mannion PD, Sullivan C, Upchurch P, Evans SE.
712 2014. Rates of dinosaur body mass evolution indicate 170 million years of sustained
713 ecological innovation on the avian stem lineage. *PloS Biology* 12:e1001853.
714 Berge C, Penin X. 2004. Ontogenetic allometry, heterochrony, and interspecific differences in
715 the skull of african apes, using tridimensional procrustes analysis. *American Journal of*
716 *Physical Anthropology* 124:124–138.
717 Bever GS, Norell MA. 2009. The perinate skull of *Byronosaurus* (Troodontidae) with
718 observations on the cranial Ontogeny of paravian theropods. *American Museum Novitates*
719 3657:1–51.
720 Bhullar B-A, Marugán-Lobón J, Racimo F, Bever GS, Rowe TB, Norell MA, Abzhanov A.
721 2012. Birds have paedomorphic dinosaur skulls. *Nature* 487:223–226.
722 Bhullar B-A. 2012. A phylogenetic approach to ontogeny and heterochrony in the fossil record:
723 cranial evolution and development in anguimorphan lizards (Reptilia: Squamata). *Journal*
724 *of Experimental Zoology (MOL DEV EVOL)* 318B:521–530.
725 Bonnan MF. 2004. Morphometric analysis of humerus and femur shape in Morrison sauropods:
726 implications for functional morphology and paleobiology. *Paleobiology* 30:444–470.
727 Bookstein FL. 1991. *Morphometric tools for landmark data*. Cambridge: Cambridge University
728 Press.
729 Bookstein FL, Schäfer K, Prossinger H, Seidler H, Fiedler M, Stringer C, Weber GW, Arsuaga J-
730 L, Slice DE, Rohlf FJ, Recheis W, Mariam AJ, Marcus LF. 1999. Comparing frontal
731 cranial profiles in archaic and modern *Homo* by morphometric analysis. *The Anatomical*
732 *Record* 257:217–224.

733 Brown CM, Evans DC, Campione NE, O’ Brien LJ, Eberth DA. 2013. Evidence for taphonomic
734 size bias in the Dinosaur Park Formation (Campanian, Alberta), a model Mesozoic
735 terrestrial alluvial‐paralic system. *Palaeogeography, Palaeoclimatology, Palaeoecology*
736 372:108–122.
737 Brown CM, Vavrek MJ. 2015. Small sample sizes in the study of ontogenetic allometry;
738 implications for palaeobiology. *PeerJ* 3:e818.
739 Brusatte SL, Benton MJ, Ruta M, Lloyd GT. 2008. Superiority, competition, and opportunism in
740 the evolutionary radiation of dinosaurs. *Science* 321:1485–1488.
741 Brusatte SL, Norell MA, Carr TD, Erickson GM, Hutchinson JR, Balanoff AM, Bever GS,
742 Choiniere JN, Makovicky PJ, Xu X. 2010. Tyrannosaur paleobiology: new research on
743 ancient exemplar organisms. *Science* 329:1481–1485.
744 Brusatte SL. 2011. Calculating the tempo of morphological evolution: rates of discrete character
745 change in a phylogenetic context. In: Elewa AMT ed. *Computational Paleontology*.
746 Heidelberg: Springer, 53–74.
747 Brusatte SL, Montanari S, Sakamoto M, Harcourt-Smith WEH. 2012. The evolution of cranial
748 form and function in theropod dinosaurs: insight from geometric morphometrics. *Journal*
749 *of Evolutionary Biology* 25:365–377.
750 Bybee PJ, Lee AH, Lamm E-T. 2006. Sizing the Jurassic theropod dinosaur *Allosaurus*:
751 assessing growth strategy and evolution of ontogenetic scaling of limbs. *Journal of*
752 *Morphology* 267:347–359.
753 Cabreira SF, Schultz CL, Bittencourt JS, Soares MB, Fortier DC, Silva LR, Langer MC. 2011.
754 New stem-sauropodomorph (Dinosauria, Saurischia) from the Triassic of Brazil.
755 *Naturwissenschaften* 98:1035–1040.

Campione NE, Evans DC. 2011. Cranial growth and variation in edmontosaurs (Dinosauria: Hadrosauridae): implications for Latest Cretaceous megaherbivore diversity in North America. *PLoS ONE* 6:e25186.

Canale IC, Novas FE, Salgado L, Coria RA. 2014. Cranial ontogenetic variation in *Mapusaurus roseae* (Dinosauria: Theropoda) and the probable role of heterochrony in carcharodontosaurid evolution. *Paläontolologische Zeitschrift*:1–11.

Cardini A, Elton S. 2007. Sample size and sampling error in geometric morphometric studies of size and shape. *Zoomorphology* 126:121–134.

Carr TD. 1999. Craniofacial ontogeny in Tyrannosauridae (Dinosauria, Coelurosauria). *Journal of Vertebrate Paleontology* 19:497–520.

Carrano MT, Benson RBJ, Sampson SD. 2012. The phylogeny of Tetanurae (Dinosauria: Theropoda). *Journal of Systematic Palaeontology* 10:211–300.

Chinnery B. 2004. Morphometric analysis of evolutionary trends in the ceratopsian postcranial skeleton. *Journal of Vertebrate Paleontology* 24:591–609.

Colbert EH. 1989. The Triassic dinosaur *Coelophysis*. *Museum of Northern Arizona Bulletin* 57: 1–160.

Colbert EH. 1990. Variation in *Coelophysis bauri*. In: Carpenter K, Currie PJ eds. *Dinosaur systematics: approaches and perspectives*. Cambridge: Cambridge University Press, 81–90.

Collyer ML, Adams DC. 2007. Analysis of two-state multivariate phenotypic change in ecological studies. *Ecology* 88:683–692.

Corti M. 1993. Geometric Morphometrics: an extension of the revolution. *Trends in Ecology and Evolution* 8:302–303.

779 Cumming G, Fidler F, Vaux DL. 2007. Error bars in experimental biology. *The Journal of Cell*
780 *Biology* 177:7–11.
781 Currie PJ, Chen P. 2001. Anatomy of *Sinosauropteryx prima* from Liaoning, northeastern China.
782 *Canadian Journal of Earth Sciences* 38:1705–1727.
783 Dal Sasso C, Maganuco S. 2011. *Scipionyx samniticus* (Theropoda: Compsognathidae) from the
784 Lower Cretaceous of Italy. *Memorie della Società Italiana di Scienze Naturali e del Museo*
785 *Civico di Storia Naturale di Milano* 37:1–281.
786 Dececchi TA, Larsson HCE. 2013. Body and limb size dissociation at the origin of birds:
787 uncoupling allometric constraints across a macroevolutionary transition. *Evolution*
788 67:2741–2752.
789 Drake AG. 2011. Dispelling dog dogma: an investigation of heterochrony in dogs using 3D
790 geometric morphometric analysis of skull shape. *Evolution & Development* 13:204–213.
791 Erickson GM, Makovicky PJ, Currie PJ, Norell MA, Yerby SA, Brochu CA. 2004. Gigantism
792 and comparative life-history parameters of tyrannosaurid dinosaurs. *Nature* 430:772–775.
793 Ezcurra MD. 2012. Phylogenetic analysis of Late Triassic-Early Jurassic neotheropod dinosaurs:
794 implications for the early theropod radiation. *Journal of Vertebrate Paleontology, Program*
795 *and Abstracts* 32:91.
796 Ezcurra MD, Butler RJ. 2015. Post-hatchling cranial ontogeny in the Early Triassic diapsid
797 reptile *Proterosuchus fergusi*. *Journal of Anatomy*:1–16.
798 Ezcurra MD, Novas FE. 2007. Phylogenetic relationships of the Triassic theropod *Zupaysaurus*
799 *rougieri* from NWArgentina. *Historical Biology* 19:35–72.

800 Forasiepi AM, Sánchez-Villagra MR. 2014. Heterochrony, dental ontogenetic diversity, and the
801 circumvention of constraints in marsupial mammals and extinct relatives. *Paleobiology*
802 40:222–237.
803 Foth C, Rauhut OWM. 2013a. Macroevolutionary and morphofunctional patterns in theropod
804 skulls: a morphometric approach. *Acta Palaeontologica Polonica* 58:1–16.
805 Foth C, Rauhut OWM. 2013b. The good, the bad, and the ugly: the influence of skull
806 reconstructions and intraspecific variability in studies of cranial morphometrics in
807 theropods and basal saurischians. *PLoS ONE* 8:e72007.
808 Gerber S, Neige P, Eble GJ. 2007. Combining ontogenetic and evolutionary scales of
809 morphological disparity: a study of early Jurassic ammonites. *Evolution & Development*
810 9:472–482.
811 Gower JC. 1975. Generalized Procrustes analysis. *Psychometrika* 40:33–51.
812 Guenther MF. 2009. Influence of sequence heterochrony on hadrosaurid dinosaur postcranial
813 development. *The Anatomical Record* 292:1427–1441.
814 Hedrick BP, Dodson P. 2013. Lujiatun psittacosaurids: understanding individual and taphonomic
815 variation using 3D geometric morphometrics. *PLoS ONE* 8:e69265.
816 Henderson DM. 2002. The eyes have it: the sizes, shapes, and orientations of theropod orbits as
817 indicators of skull strength and bite force. *Journal of Vertebrate Paleontology* 22:766–778.
818 Henderson DM, Weishampel DB. 2002. Convergent evolution of the maxilla-dental-complex
819 among carnivorous archosaurs. *Senckenbergiana lethaea* 82:77–92.
820 Hendrickx C, Mateus O. 2014. Abelisauridae (Dinosauria: Theropoda) from the Late Jurassic of
821 Portugal and dentition-based phylogeny as a contribution for the identification of isolated
822 theropod teeth. *Zootaxa* 3759:1–74.

Hennig W. 1966. *Phylogenetic systematics*. Urbana: University of Illinois Press.

Hone DWE, Naish D, Cuthill I. 2012. Does mutual sexual selection explain the evolution of head crests in pterosaurs and dinosaurs? *Lethaia* 45:139–156.

Hone DWE, Rauhut OWM. 2010. Feeding behaviour and bone utilization by theropod dinosaurs. *Lethaia* 43:232–244.

Irmis RB. 2011. Evaluating hypotheses for the early diversification of dinosaurs. *Earth and Environmental Science Transactions of the Royal Society of Edinburgh* 101:397–426.

Jackson DA. 1993. Stopping rules in principal components analysis: a comparison of heuristical and statistical approaches. *Ecology* 74:2204–2214.

Klingenberg CP. 1998. Heterochrony and allometry: the analysis of evolutionary change in ontogeny. *Biological Reviews* 73:79–123.

Klingenberg CP. 2011. MorphoJ: an integrated software package for geometric morphometrics. *Molecular Ecology Resources* 11:353–357.

Klingenberg CP, Gidaszewski NA. 2010. Testing and quantifying phylogenetic signals and homoplasy in morphometric data. *Systematic Biology* 59:245–261.

Kundrát M, Cruickshank ARI, Manning TW, Nudds J. 2008. Embryos of therizinosauroid theropods from the Upper Cretaceous of China: diagnosis and analysis of ossification patterns. *Acta Zoologica (Stockholm)* 89:231–251.

Laurin M. 2004. The evolution of body size, Cope's rule and the origin of amniotes. *Systematic Biology* 53:594–622.

Lautenschlager S. 2014. Morphological and functional diversity in therizinosaur claws and the implications for theropod claw evolution. *Proceedings of the Royal Society B* 281:20140497.

Lee MSY, Cau A, Naish D, Dyke GJ. 2014. Sustained miniaturization and anatomical innovation in the dinosaurian ancestors of birds. *Science* 345:562–566.

Lieberman DE, Carlo J, Ponc de Leóon M, Zollikofer CPE. 2007. A geometric morphometric analysis of heterochrony in the cranium of chimpanzees and bonobos. *Journal of Human Evolution* 52:647–662.

Loewen MA. 2009. *Variation in the Late Jurassic theropod dinosaur* Allosaurus*: ontogenetic, functional, and taxonomic implications*. University of Utah, Salt Lake City.

Loewen MA, Irmis RB, Sertich JJW, Currie PJ, Sampson SD. 2013. Tyrant dinosaur evolution tracks the rise and fall of Late Cretaceous oceans. *PLoS ONE* 8:e79420.

Long JA, McNamara KJ. 1997. Heterochrony: the key to dinosaur evolution. In: Wolberg DL, Stumps E, Rosenberg GD eds. *Dinofest International*. Philadelphia: Academy of Natural Sciences, 113–123.

Maddison WP. 1991. Squared-change parsimony reconstructions of ancestral states for continuous-valued characters on a phylogenetic tree. *Systematic Zoology* 40:304–314.

Maddison WP, Maddison DR. 2009. Mesquite: A modular system of evolutionary analysis. Version 2.72.

Madsen JHJ, Welles SP. 2000. *Ceratosaurus* (Dinosauria, Theropoda), a revised osteology. *Utah Geology Survey Miscellaneous Publication* 00-2:1–80.

Maiorini L, Farke AA, Kotsakis T, Piras P. 2015. Males resemble females: re-evaluating sexual dimorphism in *Protoceratops andrewsi* (Neoceratopsia, Protoceratopsidae). *PLoS ONE* 10:e0126464.

867 Martínez RN. 2009. *Adeopapposaurus mognai*, gen. et sp. nov. (Dinosauria: Sauropodomorpha),
868 with comments on adaptations of basal Sauropodomorpha. *Journal of Vertebrate*
869 *Paleontology* 29:142–164.
870 Martínez RN, Sereno PC, Alcober OA, Colombi CE, Renne PR, Montañez IP, Currie BS. 2011.
871 A basal dinosaur from the dawn of the dinosaur era in southwestern Pangaea. *Science*
872 331:206–210.
873 Martínez RN, Apaldetti C, Abelin D. 2013. Basal sauropodomorphs from the Ischigualasto
874 Formation. *Society of Vertebrate Paleontology Memoir* 12:51–69.
875 McNamara KJ. 1982. Heterochrony and phylogenetic trends. *Paleobiology* 8:130–142.
876 McNamara KJ. 2012. Heterochrony: the evolution of development. *Evolution: Education and*
877 *Outreach* 5:203–218.
878 McNamara KJ, McKinney ML. 2005. Heterochrony, disparity, and macroevolution.
879 *Paleobiology* 31:17–26.
880 Mitteroecker P, Gunz P, Weber GW, Bookstein FL. 2004. Regional dissociated heterochrony in
881 multivariate analysis. *Annals of Anatomy* 186:463–470.
882 Mitteroecker P, Gunz P. 2009. Advances in geometric morphometrics. *Evolutionary Biology*
883 36:235–247.
884 Mitteroecker P, Gunz P, Bookstein FL. 2005. Heterochrony and geometric morphometrics: a
885 comparison of cranial growth in *Pan paniscus* versus *Pan troglodytes*. *Evolution &*
886 *Development* 7:244–258.
887 Molnar RE. 2005. Sexual selection and sexual dimorphism in theropods. In: Carpenter K ed. *The*
888 *carnivorous dinosaurs*. Bloomington: Indiana University Press, 284–312.

889 Norell MA, Clark JM, Turner AH, Makovicky PJ, Barsbold R, Rowe TB. 2006. A new
890 droameosaurid theropod from Ukhaa Tolgod (Ömnögov, Mongolia). *American Museum*
891 *Novitates* 3545:1–51.
892 Padian K, Horner JR. 2011. The evolution of "bizarre structures" in dinosaurs: biomechanics,
893 sexual selection, social selection or species recognition? *Journal of Zoology* 283:3–17.
894 Paradis E, Claude J, Strimmer K. 2004. APE: analyses of phylogenetics and evolution in R
895 language. *Bioinformatics* 20:289–290.
896 Peyer K. 2006. A reconsideration of *Compsognathus* from the Upper Tithonian of Canjuers,
897 southeastern France. *Journal of Vertebrate Paleontology* 26:879–896.
898 Piras P, Salvi D, Ferrara G, Maiorino L, Delfino M, Pedde L, Kotsakis T. 2011. The role of post-
899 natal ontogeny in the evolution of phenotypic diversity in *Podarcis* lizards. *Journal of*
900 *Evolutionary Biology* 24:2705–2720.
901 Pol D, Rauhut OWM. 2012. A Middle Jurassic abelisaurid from Patagonia and the early
902 diversification of theropod dinosaurs. *Proceedings of the Royal Society B* 279:3170–3175.
903 Rauhut OWM. 2003. The interrelationships and evolution of basal theropod dinosaurs. *Special*
904 *Papers in Palaeontology* 69:1–213.
905 Rauhut OWM, Fechner R, Remes K, Reis K. 2011. How to get big in the Mesozoic: the
906 evolution of the sauropodomorph body plan. In: Klein N, Remes K, Gee CT, Sander PM
907 eds. *Biology of the sauropod dinosaurs: understanding the life of giants*. Bloomington:
908 Indiana University Press, 119–149.
909 Rauhut OWM, Foth C, Tischlinger H, Norell MA. 2012. Exceptionally preserved juvenile
910 megalosauroid theropod dinosaur with filamentous integument from the Late Jurassic of
911 Germany. *Proceedings of the National Academy of Sciences* 109:11746–11751.

912 Rauhut OWM, Fechner R. 2005. Early development of the facial region in a non-avian theropod
913 dinosaur. *Proceedings of the Royal Society B* 272:1179–1183.
914 Rauhut OWM, Milner AC, Moore-Fay S. 2010. Cranial osteology and phylogenetic position of
915 the theropod dinosaur *Proceratosaurus bradleyi* (Woodward, 1910) from the Middle
916 Jurassic of England. *Zoological Journal of the Linnean Society* 158:155–195.
917 R-Development-Core-Team. 2011. R: a language and environment for statistical computing.
918 Reilly SM, Wiley EO, Meinhardt DJ. 1997. An integrative approach to heterochrony: the
919 distinction between interspecific and intraspecific phenomena. *Biological Journal of the*
920 *Linnean Society* 60:119–143.
921 Reisz RR, Evans DC, Sues H-D, Scott D. 2010. Embryonic skeletal anatomy of the
922 sauropodomorph dinosaur *Massospondylus* from the Lower Jurassic of South Africa.
923 *Journal of Vertebrate Paleontology* 30:1653–1665.
924 Rinehart LF, Lucas SG, Heckert AB, Spielmann JA, Celeskey MD. 2009. The paleobiology of
925 *Coelophysis bauri* (Cope) from the Upper Triassic (Apachean) Whitaker quarry, New
926 Mexico, with detailed analysis of a single quarry block. *New Mexico Museum of Natural*
927 *History and Science, Bulletin* 45:1–260.
928 Rohlf FJ. 2005. tpsDig, digitize landmarks and outlines, version 2.05.
929 Rohlf FJ, Marcus LF. 1993. A revolution in morphometrics. *Trends in Ecology and Evolution*
930 8:129–132.
931 Rohlf FJ, Slice DE. 1990. Extensions of the Procrustes method for the optimal superimposition
932 of landmarks. *Systematic Zoology* 39:40–59.
933 Rowe TB. 1989. A new species of the theropod dinosaur *Syntarsus* from the Early Jurassic
934 Kayenta Formation of Arizona. *Journal of Vertebrate Paleontology* 9:125–136.

935 Sampson SD. 1999. Sex and destiny: the role of mating signals in speciation and
936 macroevolution. *Historical Biology* 13:173–197.
937 Sander PM, Klein N, Buffetaut E, Cuny G, Suteethorn V, Le Loeuff J. 2004. Adaptive radiation
938 in sauropod dinosaurs: bone histology indicates rapid evolution of giant body size through
939 acceleration. *Organisms, Diversity & Evolution* 4:165–173.
940 Sander PM, Christian A, Clauss M, Fechner R, Gee CT, Griebeler EM, Gunga H-C, Hummel J,
941 Mallison H, Perry SF, Preuschoft H, Rauhut OWM, Remes K, Tüttken T, Wings O, Witzel
942 U. 2010. Biology of the sauropod dinosaurs: the evolution of gigantism. *Biological*
943 *Reviews* 86:117–155.
944 Schmitz L, Motani R. 2011. Nocturnality in dinosaurs inferred from scleral ring and orbit
945 morphology. *Science* 332:705–708.
946 Schoch RR. 2009. Life-cycle evolution as response to diverse lake habitats in Paleozoic
947 amphibians. *Evolution* 63:2738–2749.
948 Schoch RR. 2010. Heterochrony: the interplay between development and ecology exemplified by
949 a Paleozoic amphibian clade. *Paleobiology* 36:318–334.
950 Schoch RR. 2014. Amphibian skull evolution: the developmental and functional context of
951 simplification, bone loss and heterotopy. *Journal of Experimental Zoology (MOL DEV*
952 *EVOL)* 322B:619–630.
953 Schwarz-Wings D, Böhm N. 2014. A morphometric approach to the specific separation of the
954 humeri and femora of *Dicraeosaurus* from the Late Jurassic of Tendaguru/Tanzania. *Acta*
955 *Palaeontologica Polonica* 59:81–98.
956 Singleton M. 2002. Patterns of cranial shape variation in the *Papionini* (Primates:
957 Cercopithecinae). *Journal of Human Evolution* 42:547–578.

958 Slice DE. 2007. Geometric morphometrics. *Annual Review of Anthropology* 36:261–281.
959 Smith KK. 1993. The form of the feeding apparatus in terrestrial vertebrates: studies of
960 adaptation and constraint. In: Hanken J, Hall BK eds. *The skull. Vol. 3. Patterns of*
961 *structural and systematic diversity*. Chicago: University of Chicago Press, 150–196.
962 Smith ND, Makovicky PJ, Hammer WR, Currie PJ. 2007. Osteology of *Cryolophosaurus ellioti*
963 (Dinosauria: Theropoda) from the Early Jurassic of Antarctica and implications for early
964 theropod evolution. *Zoological Journal of the Linnean Society* 151:377–421.
965 Stromer E. 1934. Die Zähne des *Compsognathus* und Bemerkungen über das Gebiß der
966 Theropoda. *Centralblatt für Mineralogie, Geologie und Paläontologie, B* 1934:74–85.
967 Sues H-D, Nesbitt SJ, Berman DS, Henrici AC. 2011. A late-surviving basal theropod dinosaur
968 from the latest Triassic of North America. *Proceedings of the Royal Society B* 278:3459–
969 3464.
970 Therrien F, Henderson DM. 2007. My theropod is bigger than yours...or not: estimating body
971 size from skull length in theropods. *Journal of Vertebrate Paleontology* 27:108–115.
972 Tsuihiji T, Watabe M, Tsogtbaatar K, Tsubamoto T, Barsbold R, Suzuki S, Lee AH, Ridgely
973 RC, Kawahara Y, Witmer LM. 2011. Cranial osteology of a juvenile specimens of
974 *Tarbosaurus bataar* (Theropoda, Tyrannosauridae) from the Nemegt Formation (Upper
975 Cretaceous) of Bugin Tsav, Mongolia. *Journal of Vertebrate Paleontology* 31:497–517.
976 Turner AH, Makovicky PJ, Norell MA. 2012. A review of dromaeosaurid systematics and
977 paravian phylogeny. *Bulletin of the American Museum of Natural History* 371:1–206.
978 Tykoski RS. 1998. *The osteology of* Syntarsus kayentakatae *and its implications for ceratosaurid*
979 *phylogeny*. Austin: The University of Texas, Austin.

980 Wilson JA, Sereno PC. 1998. Early evolution and higher-level phylogeny of sauropod dinosaurs.
981 *Society of Vertebrate Paleontology Memoir* 5:1–68.
982 Witmer LM. 1997. The evolution of the antorbital cavity of archosaurs: a study in soft-tissue
983 reconstruction in the fossil record with an analysis of the function of pneumaticity. *Society*
984 *of Vertebrate Paleontology Memoir* 3:1–73.
985 Witzel U, Mannhardt J, Goessling R, Micheeli P, Preuschoft H. 2011. Finite element analyses
986 and virtual syntheses of biological structures and their application to sauropod skulls. In:
987 Klein N, Remes K, Gee CT, Sander PM eds. *Biology of the sauropod dinosaurs:*
988 *understanding the life of giants*. Bloomington: Indiana University Press, 171–181.
989 Witzel U, Preuschoft H. 2005. Finite-element model construction for the virtual synthesis of the
990 skulls in vertebrates: case study of Diplodocus. *The Anatomical Record* 283A:391–401.
991 Xu X, Norell MA, Kuang X, Wang X, Zhao Q, Jia C. 2004. Basal tyrannosauroids from China
992 and evidence for protofeathers in tyrannosauroids. *Nature* 431:680–684.
993 Xu X, Clark JM, Forster CA, Norell MA, Erickson GM, Eberth DA, Jia C, Zhao Q. 2006. A
994 basal tyrannosauroid dinosaur from the Late Jurassic of China. *Nature* 439:715–718.
995 Xu X, Wu X. 2001. Cranial morphology of *Sinornithosaurus millenii* Xu et al. 1999 (Dinosauria:
996 Theropoda: Dromaeosauridae) from the Yixian Formation of Liaoning, China. *Canadian*
997 *Journal of Earth Sciences* 38:1739–1752.
998 Young MT, Larvan MD. 2010. Macroevolutionary trends in the skull of sauropodomorph
999 dinosaurs - the largest terrestrial animals to have ever lived. In: Elewa AMT ed.
1000 *Morphometrics for non-morphometricans*. Berlin: Springer, 259–269.

1001 Zanno LE, Makovicky PJ. 2011. Herbivorous ecomorphology and specialization patterns in
1002 theropod dinosaur evolution. *Proceedings of the National Academy of Sciences* 108:232–
1003 237.
1004 Zelditch ML, Swiderski DL, Sheets HD. 2012. *Geometric morphometrics for biologists: a*
1005 *primer*. Amsterdam: Elsevier Academic Press.
1006

1008 **Figure and Table captions**

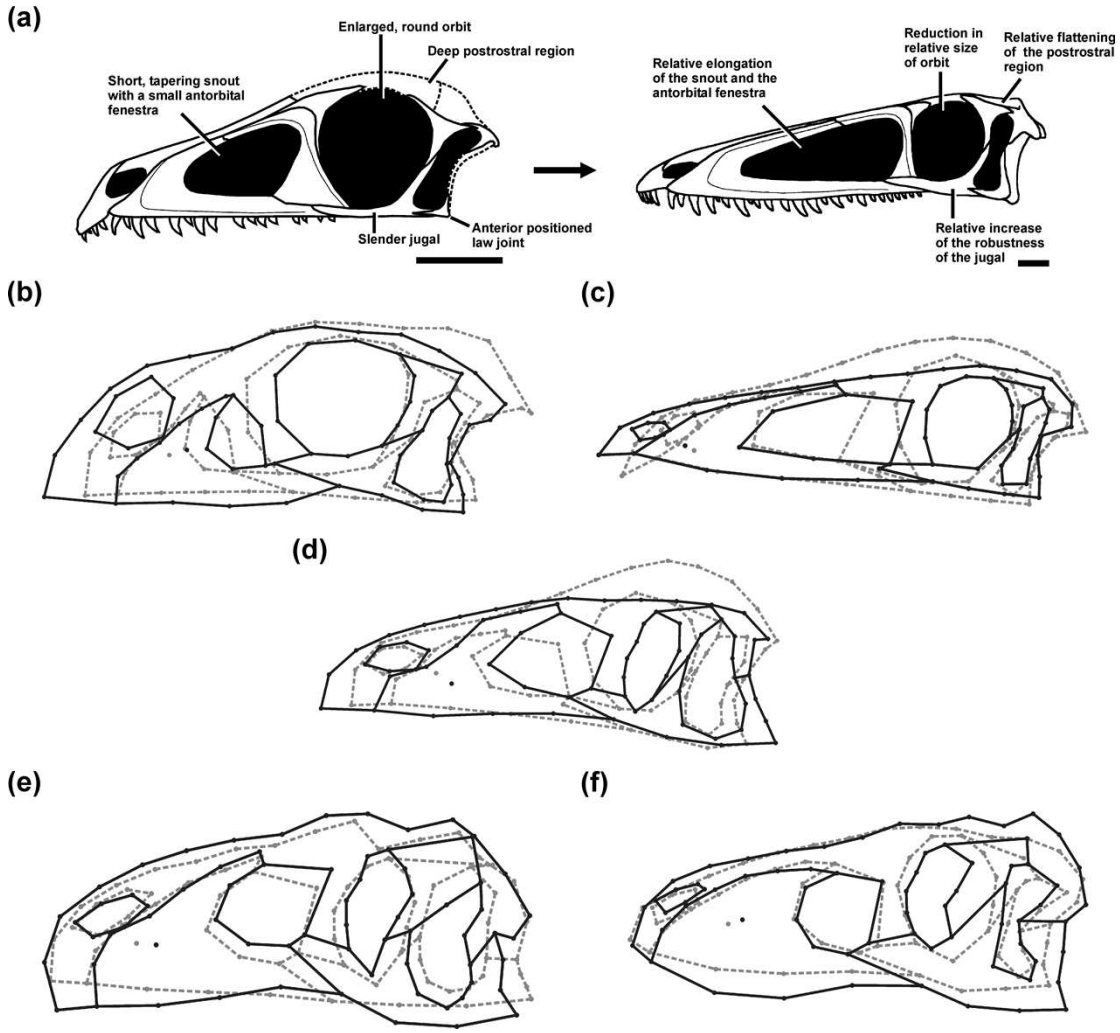

1009

1010 **Figure 1 Ontogenetic changes in saurischian dinosaurs**. (a) General ontogenetic pattern in

1011 Saurischia exemplified for *Coelophysis* (adult specimen modified after Rauhut, 2003). (b-f)

1012 Specific ontogenetic changes in saurischian dinosaurs visualized as wireframes of Procrustes

1013 shapes. (b) *Massospondylus*. (c) *Coelophysis*. (d) Megalosaurid taxon. (e) *Allosaurus*. (f)

1014 *Tarbosaurus*. Grey dashed lines represent the juvenile stage and black solid lines represent the

1015 adult stage.

1016

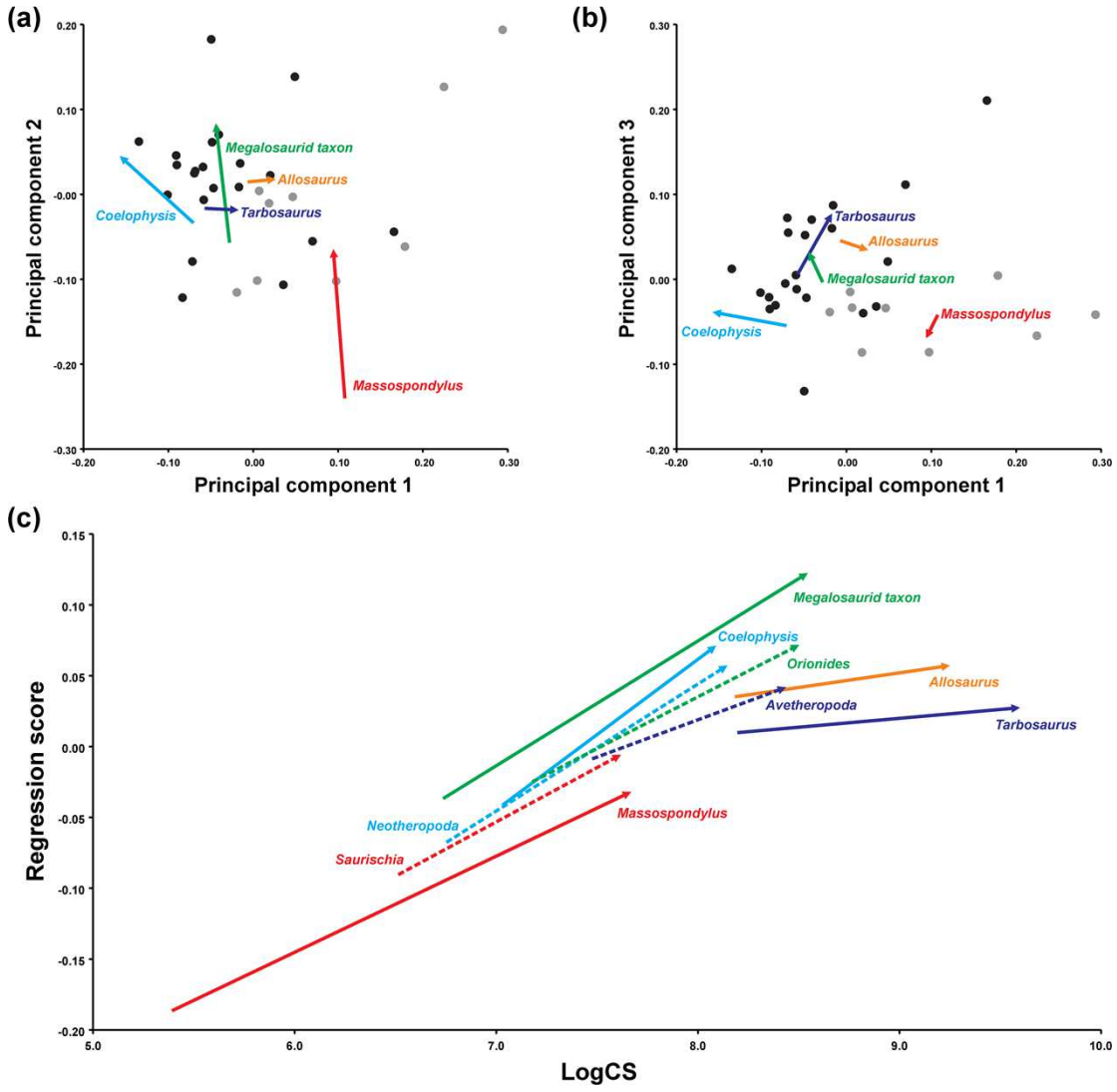

1017

1018 **Figure 2 PCA and regression analysis of the main sample**. (a) Ontogenetic trajectories of

1019 terminal taxa for PC 1 versus PC 2. (b) Ontogenetic trajectories of terminal taxa for PC 1 against

1020 PC 3. Theropod taxa are shown as black dots, while sauropodomorph taxa are shown as grey

1021 dots. (c) Regression analysis against log-transformed skull centroid size (LogCS) showing the

1022 ontogenetic trajectories of saurischian dinosaurs based on the overall skull Procrustes shapes of

1023 terminal taxa (solid lines) and hypothetical ancestors (dashed lines).

1024

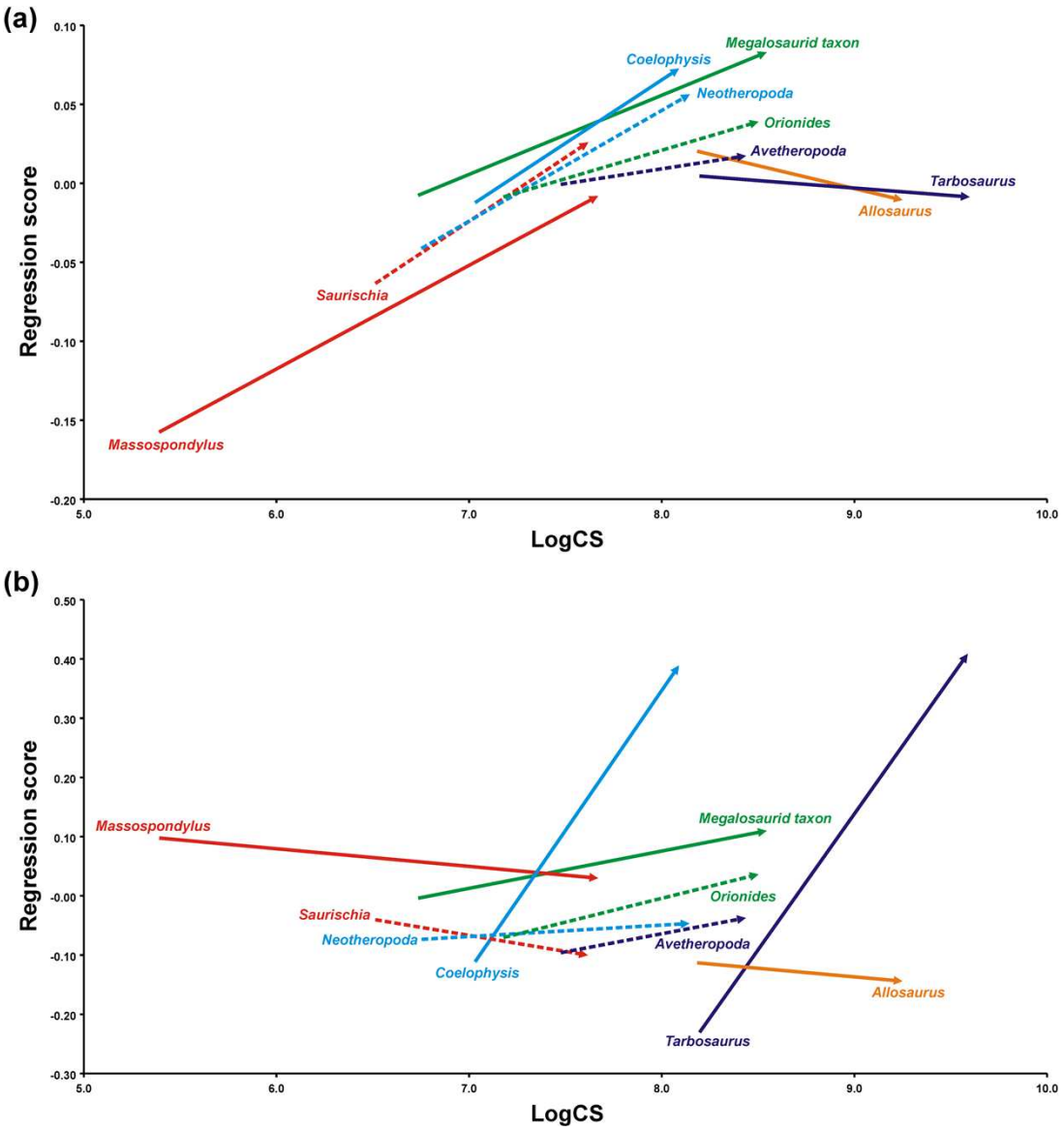

Figure 3 Regression analyses for the skull outline and the external naris. Ontogenetic trajectories of terminal taxa (solid lines) and hypothetical ancestors (dashed lines) against log-transformed skull centroid size (LogCS). (a) Shape of the skull outline. (b) Shape of the external naris.

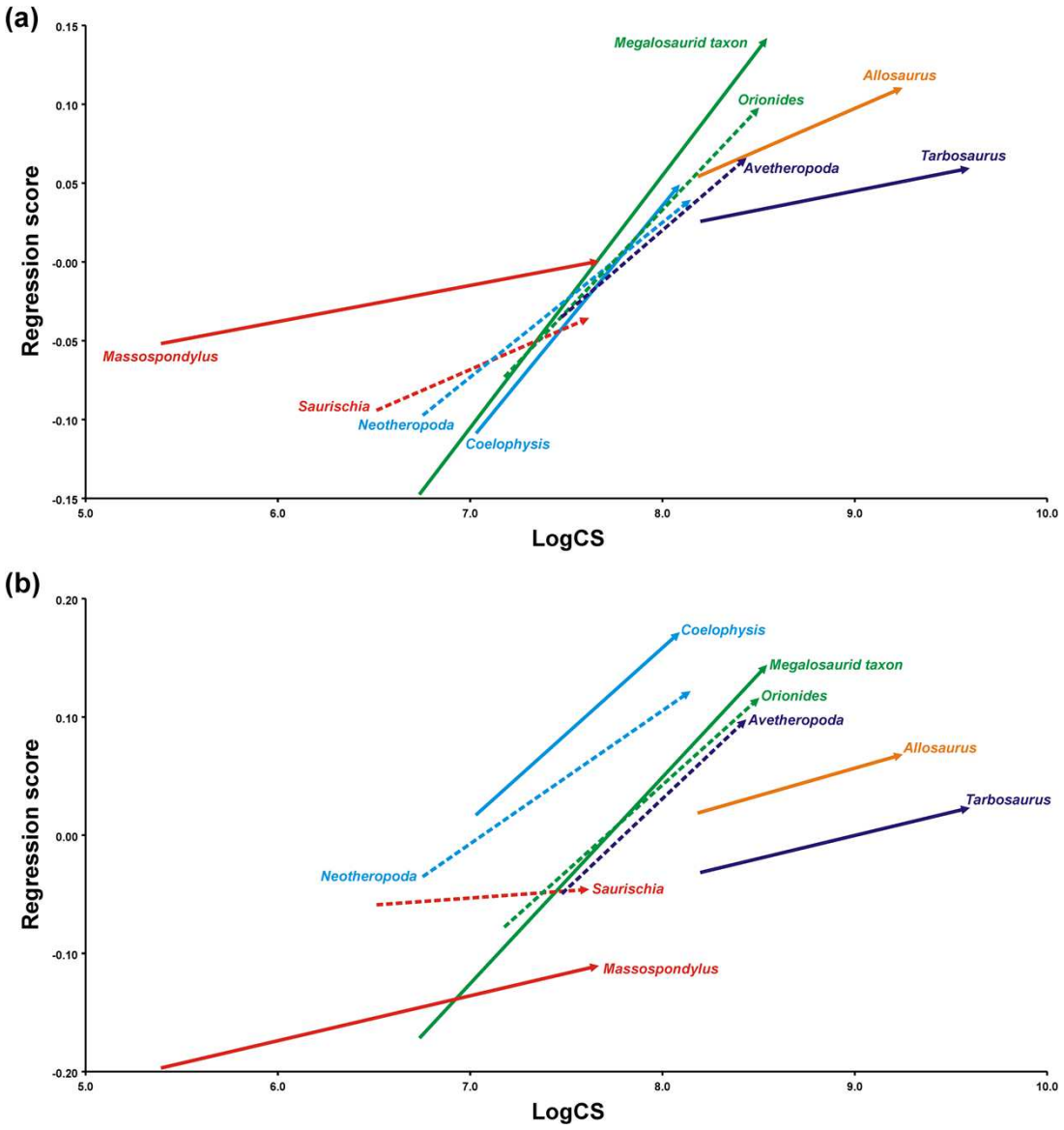

1031

1032 **Figure 4 Regression analyses for the maxilla and antorbital fenestra.** Ontogenetic trajectories

1033 of terminal taxa (solid lines) and hypothetical ancestors (dashed lines) against log-transformed

1034 skull centroid size (LogCS). (a) Shape of the maxilla. (b) Shape of the antorbital fenestra.

1035

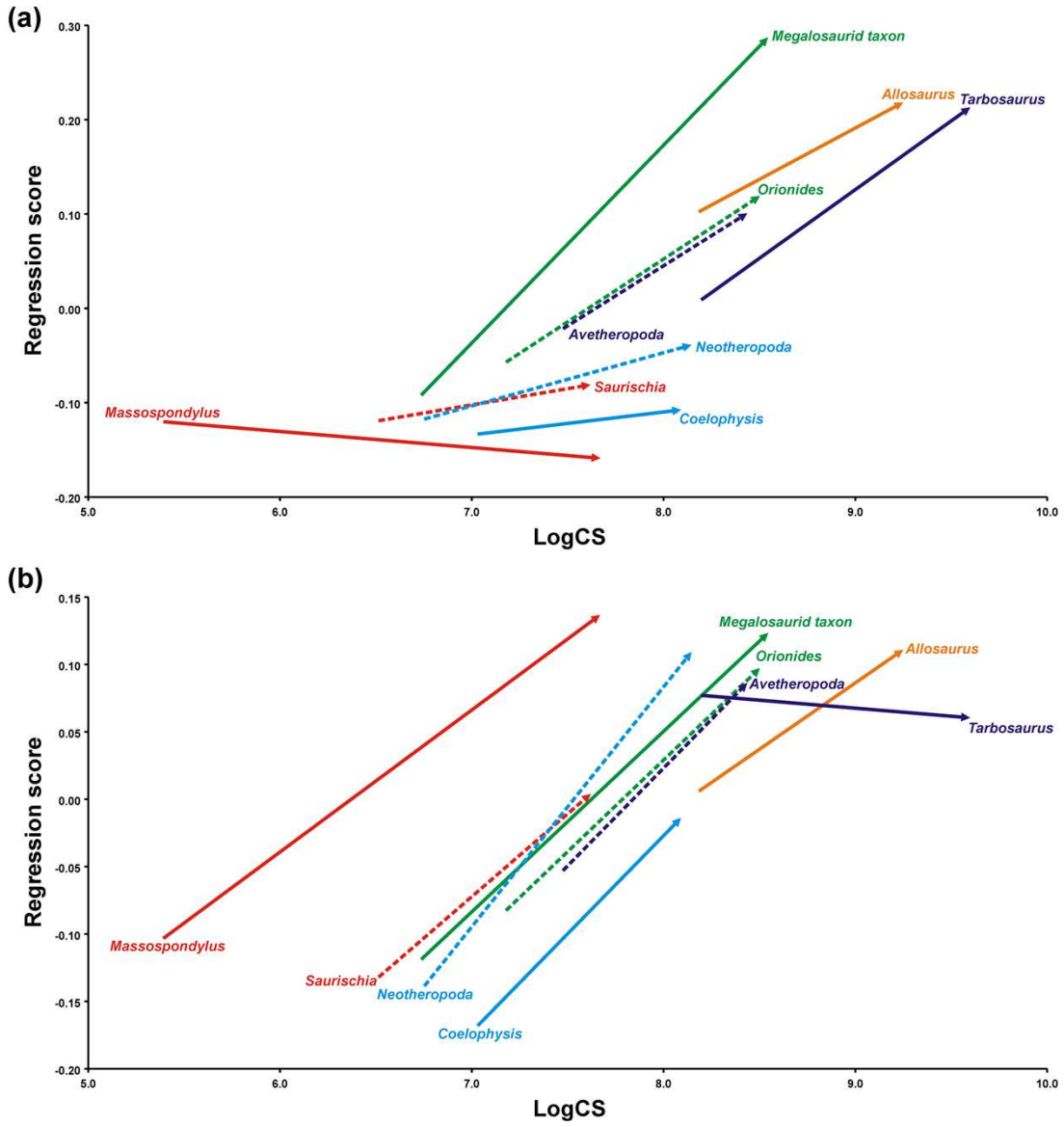

1036

1037 **Figure 5 Regression analyses for the orbit and infratemporal fenestra.** Ontogenetic

1038 trajectories of terminal taxa (solid lines) and hypothetical ancestors (dashed lines) against log-

1039 transformed skull centroid size (LogCS). (a) Shape of the orbit. (b) Shape of the infratemporal

1040 fenestra.

1041

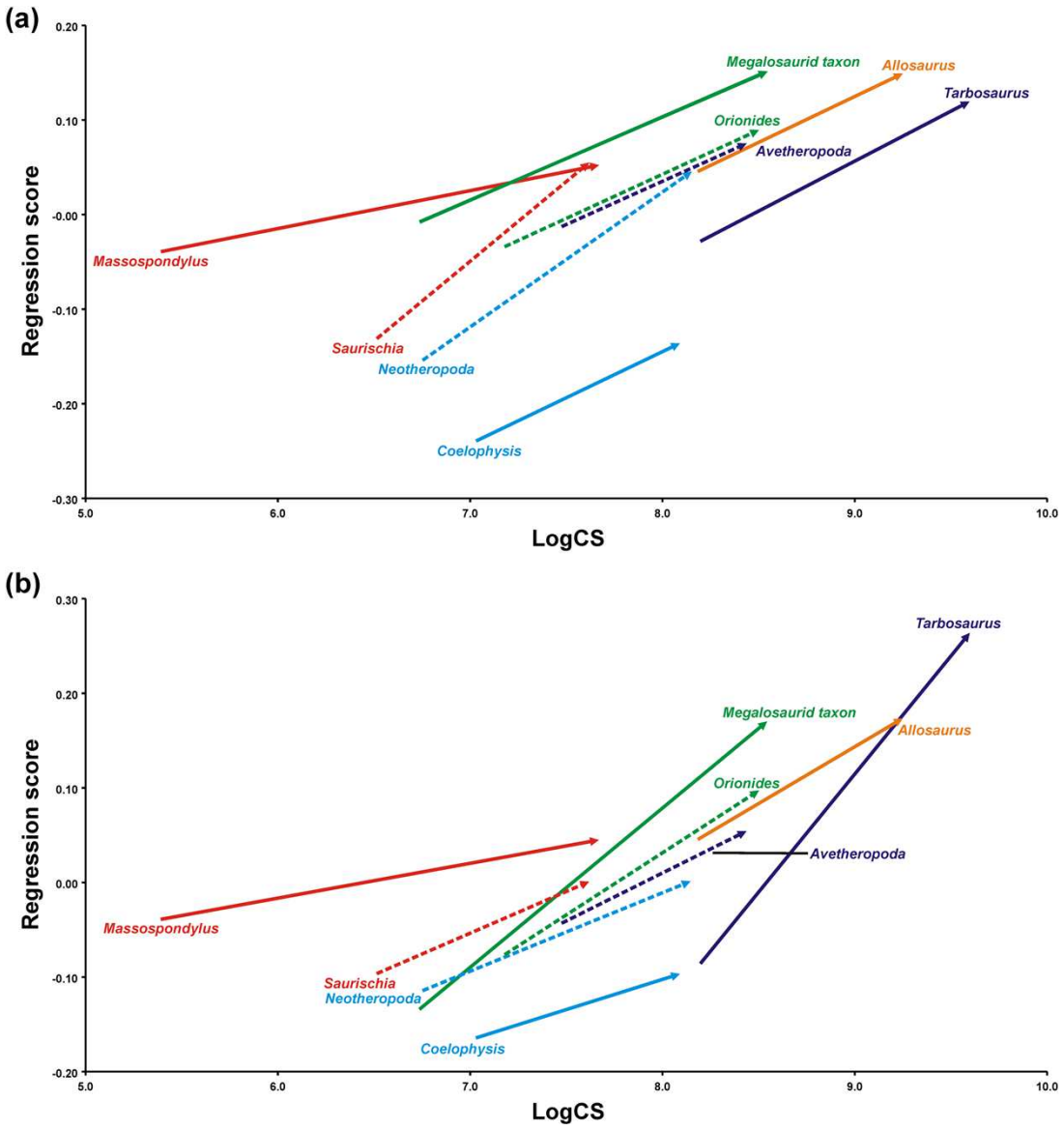

1042

1043 **Figure 6 Regression analyses for jugal-quadratojugal region and postorbital.** Ontogenetic

1044 trajectories of terminal taxa (solid lines) and hypothetical ancestors (dashed lines) against log-

1045 transformed skull centroid size (LogCS). (a) Shape of the jugal-quadratojugal region. (b) Shape

1046 of the postorbital.

1047

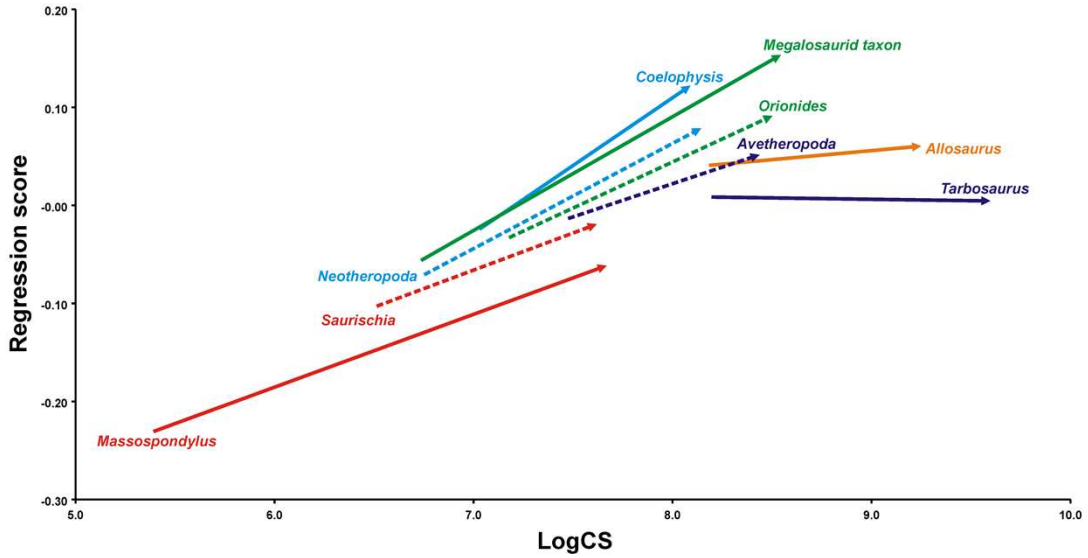

1048

1049 **Figure 7 Regression analyses for the skull roof.** Ontogenetic trajectories of terminal taxa (solid

1050 lines) and hypothetical ancestors (dashed lines) against log-transformed skull centroid size

1051 (LogCS).

1052

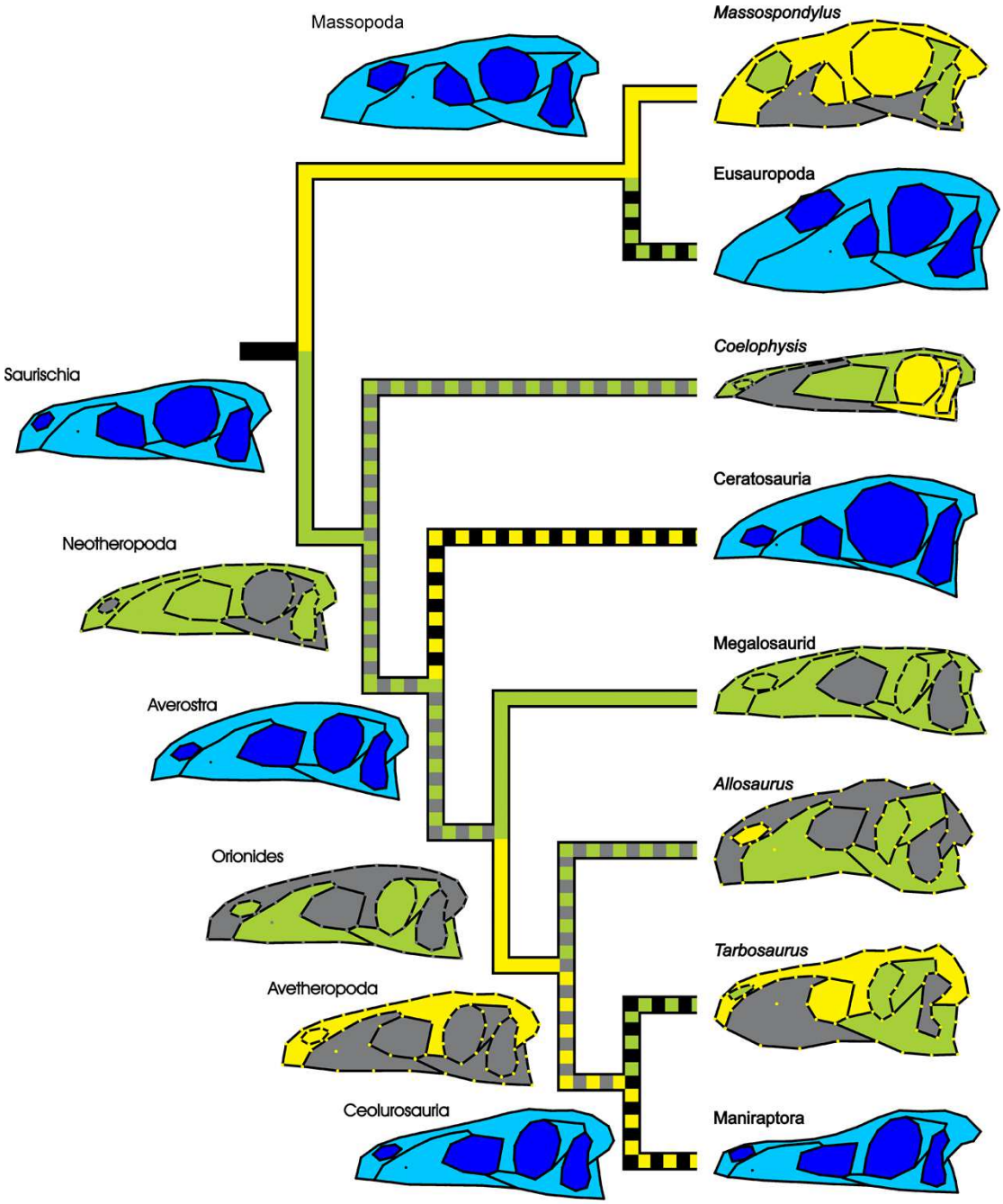

1053

1054 **Fig 8 Simplified phylogeny of Saurischia showing the main heterochronic trends of the**

1055 **overall skull shape and single skull regions.** Peramorphosis is colored in green and

1056 paedomorphosis in yellow. Shape of the hypothetical ancestors based on the continuous

1057 character mapping of the Procrustes shapes of the adult terminal taxa from the original data set.

1058 Blue skulls represent ancestral skull shapes for which ontogeny could not be analysed.

Heterochronic trends of the skull outline are visualized by the colour of the dots representing the positions of the landmarks and semi-landmarks. Grey skull regions and grey dashed branches represent evolutionary shape changes of skull regions that are not significantly different from the respective ancestor. Black dashed branches show hypothetical heterochronic trends (see discussion).

Table 1 Overview of heterochronies in saurischian overall skull shape and specific skull regions based on the regression analyses. The table shows the differences of Procrustes distances (ΔPD) between ancestor-descendent relationships of adult species. Positive values = peramorphic trends; negative values = paedomorphic trends; values in brackets = non-significant trends; AOF, antorbital fenestra; ITF, infratemporal fenestra; JU, jugal; QU, quadratojugal.

	Overall skull	Skull outline	Naris	Maxilla	AOF
Saurischia-*Massospondylus*	-0.0262**	-0.0340**	0.1295*	(0.0359)	-0.0647**
Saurischia-Neotheropoda	0.0629*	0.0304*	(0.0533)	0.0748*	0.1675*
Neotheropoda-*Coelophysis*	(0.0140)	(0.0164)	0.4359*	(0.0098)	0.0498*
Neotheropoda-Orionides	(0.0146)	(-0.0172)	0.0832*	0.0585*	(-0.0059)
Orionides-megalosaurid taxon	0.0507*	0.0437*	0.0732*	0.0442*	(0.0282)
Orionides-Avetheropoda	-0.0299**	-0.0217**	-0.0736**	(-0.0318)	(-0.0181)
Avetheropoda-*Allosaurus*	(0.0153)	-0.0280**	-0.1067**	0.0445*	(-0.0296)
Avetheropoda-*Tarbosaurus*	(-0.0145)	-0.0260**	0.4429*	(-0.0066)	-0.0748**
95 % CIs	0.01497	0.01271	0.03776	0.02723	0.02938
Significance levels (p=0.05)	0.02246	0.01907	0.05663	0.04085	0.04407

	Orbit	ITF	JU-QJ region	Postorbital	Skull roof
Saurischia-*Massospondylus*	-0.0780**	0.1328*	(-0.0029)	(0.0440)	-0.0425**
Saurischia-Neotheropoda	(0.0422)	0.1053*	(-0.0084)	(0.0004)	0.0976*
Neotheropoda-*Coelophysis*	-0.0689**	-0.1231**	-0.1827**	-0.0980**	(0.0436)
Neotheropoda-Orionides	0.1580*	(-0.0119)	0.0427*	0.0960*	0.0129*
Orionides-megalosaurid taxon	0.1681*	(0.0261)	0.0621*	0.0730*	0.0622*
Orionides-Avetheropoda	(-0.0183)	(-0.0111)	(-0.0143)	(-0.0431)	-0.0397**
Avetheropoda-*Allosaurus*	0.1176*	(0.0248)	0.0741*	0.1193*	(0.0088)
Avetheropoda-*Tarbosaurus*	0.1122*	(-0.0257)	0.0445*	0.2097*	-0.0471**
95 % CIs	0.03675	0.03044	0.02146	0.03208	0.01898
Significance levels (p=0.05)	0.05512	0.04567	0.03219	0.04812	0.02847